"The Synthesis of Light Hydrocarbons from CO and H_2
Mixtures over Selected Metal Catalysts"

M. K. Zaman Khan, Chen-Hsyong Yang, and A. G. Oblad

Department of Mining, Metallurgical and Fuels Engineering
University of Utah, Salt Lake City, Utah 84112

INTRODUCTION

The synthesis of hydrocarbons and oxygen containing organic chemicals by
reaction of CO and H_2 over catalysts has been investigated extensively in the past.
This work is summarized in a number of review papers (1-4). More recently a number
of workers have been active in investigation of these reactions (5-9). In this
extensive previous literature no particular emphasis was given to the preferential
production of lower molecular weight hydrocarbons. Mostly the previous work has
been concerned with the formation of methane and C_5^+ hydrocarbons and oxygenated
derivatives. There is an exception to this in the extensive work done in Germany
on isobutylene production in the Isosynthesis Process (10).

It, therefore, was thought to be worthwhile to reinvestigate the possibilities
for the specific production of C_2-C_4 materials with de-emphasis on the production
of CH_4 and C_5^+ substances or their elimination as products, if possible. This route
might open up new sources of C_2-C_4 hydrocarbons for use in the important petrochem-
ical industry which in recent years has been moving in the direction of heavier feed
stocks to meet the demands for ethylene, propylene and C_4 hydrocarbons (11).

This paper is a first of a series of publications from this laboratory on the
production of C_2-C_4 hydrocarbons from CO/H_2 mixtures and deals with exploratory
research on a variety of known Fischer-Tropsch catalysts. Using the literature as
a guide a number of catalysts were prepared and tested. Reaction conditions,
temperature, pressure, gas flow rate and H_2/CO ratio of the feed gas were prelimin-
arily investigated to select the most promising regime for study of the chosen
catalysts. The catalysts chosen for testing were Fe, Co, Ni, Cu, and ThO_2. The
catalysts preparation, testing procedures and the results obtained are presented in
this paper.

EXPERIMENTAL

I. Catalyst

The catalysts tested in these studies were prepared by coprecipitation and
impregnation methods. Compositions of the catalysts are based on the quantities
of metal salts used in the preparation assuming complete precipitation or in the
case of impregnation, complete adsorption of the aqueous solutions used. More
complete compositional analysis of the catalysts are now being done by analytical
methods. Table (I) contains information on the catalysts tested.

II. Description of Catalyst Testing Equipment

The reactor flow diagram is shown in Figure 1. Carbon monoxide-H_2 mixtures
prepared by Linde Speciality Gas Division of Union Carbide Co., were used. The
H_2/CO ratios were 1/1, 3/2, 2/1, 7/3, and 3/1.

The reactor was made of 314 stainless steel tubing, one foot long having an
outside diameter of 1 inch and an inside diameter of 0.5 inch. A 1-inch thick
aluminum shield was placed around the reactor tube to insure even temperature dis-
tribution in the reactor. Catalysts were loaded in the middle section of the
reactor tube and ceramic spacers were used before and after the catalysts bed. One
thermocouple was used to measure the catalyst bed temperature and another thermocouple
was used to measure the temperature of the aluminum shield. The thermocouple in the
aluminum shield was connected to a temperature controller. There was less than an
$0.5°C$ difference between the two measured temperatures when the reaction conditions

reached equilibrium.

The catalysts were oven dried at 110° C, ground to pass through a 200-mesh sieve and then tabletted into pellets. These pellets were later crushed to -14, +25 mesh size before loading in the reactor. The reaction variables were adjusted to the desired temperature, pressure, and input flow rate prior to sampling of products. Gas samples were taken at appropriate times and injected directly into chromatograph columns for analysis.

III. Analysis and Calculation of Results

A molecular sieve 5A column was used to analyze H_2, N_2, CO and CH_4. Silica gel was used to analyze H_2, CO_2 and C_2H_6. An activated alumina column with F.I.D. was used to analyze light hydrocarbons (12). A carbowax 1500-teflon column was used to analyze water and alcohols. An OV-17 column was used to analyze liquid hydrocarbons. Liquid condensate was captured in a cyclone separator and a room temperature collector. Reaction conditions were adjusted to minimize production of liquid hydrocarbons. At times small amounts were produced; these were recovered and analyzed. The C_5^+ fraction was analyzed using an activated alumina column as the G.C. oven was heated up to 370° C. These products came out in sequence of carbon atom number, the amounts decreasing with molecular weight.

Calculation of an accurate material balance was not possible since we did not have integrator equipment on the input flow. Consequently, all calculations are on an output basis. This will lead to small errors only since considerable care was taken to obtain complete recovery and accurate analysis on the product. Calculations of conversion and selectivities were done by computer on the basis of carbon atom balance. Water was collected as a liquid product but was not included in the conversion or selectivity calculations. At a later date water will be included in the analysis when material balances are possible.

CO conversions were calculated in the following manner:

All components were on a molar volume basis.

$$X = CO + CO_2 + \sum_{i=1}^{10} iC_iH_{2i+2} + \sum_{i=2}^{10} iC_iH_{2i} + \Sigma \text{ alcohols}$$

(all in the product gas)

$$Y = CO_2 + \sum_{i=1}^{10} iC_iH_{2i+2} + \sum_{i=2}^{10} iC_iH_{2i} + \Sigma \text{ alcohols}$$

(all in product gas)

$$C_5^+ = \sum_{i=5}^{10} i\,C_iH_{2i+2} + \sum_{i=5}^{10} i\,C_iH_{2i}$$

CO conversion % $= \dfrac{Y}{X} \times 100$

Selectivities for different product fractions are calculated as:

$$CO_2\% = \frac{CO_2 \text{ in product gas}}{Y} \times 100$$

$$CH_4\% = \frac{CH_4 \text{ in product gas}}{Y} \times 100$$

$$C_2\text{-}C_4 = \frac{C_2\text{-}C_4 \text{ in product gas}}{Y} \times 100$$

$$C_5^+ \% = \frac{C_5^+ \text{ in product gas}}{Y} \times 100$$

$$O/P = \frac{C_2H_4\% \times 2 + C_3H_6\% \times 3 + (1C_4H_8\% + 2C_4H_8\% + i\,C_4H_8\%) \times 4}{C_2H_6\% \times 2 + C_3H_8\% \times 3 + (nC_4H_{10}\% + i\,C_4H_{10}\%) \times 4} \times 100$$

$$R\text{-}OH\% = \frac{\Sigma \text{ alcohols in product gas}}{Y} \times 100$$

The composition analyses carried out and calculated as described are thought to be quite reliable. At the present state of development the reproducibility and accuracy of the results are estimated to be within ± 3-5 units on the percentages given.

RESULTS AND DISCUSSION

While the literature dealing with carbon monoxide hydrogenolysis is quite voluminous on the metals we have chosen for study, it is difficult if not impossible to determine their relative effectiveness for the particular products of interest in our research. Also catalysts of interest for our purposes are all not commercially available so it was necessary to synthesize our own as well as use commercially available catalysts. Likewise, the literature of Fischer-Tropsch is a rough guide only in choice of reaction conditions for our studies. It was necessary to carry out a number of preliminary studies to orient our program to suitable temperatures, pressures, H_2/CO ratios and flow rates. The synthesis is highly exothermic, consequently conversion rate must be adjusted so that temperature rise is not excessive in small catalyst bed. Temperature proved to be the most important variable influencing conversion and once the temperature range was set the ranges of the other variables were chosen not only for processing reasons but also for convenience in experimentation, handling of materials and minimizing the use of feed gases.

Iron Catalyst

Referring to Table II a number of conclusions are apparent. Iron catalysts after proper reduction and nitriding are very active for reduction of CO at the conditions chosen. Catalyst 26 was so active that the temperature of the catalyst rose to 260° C instead of 225° C which was intended at the beginning of the run. These catalysts give low methane production relative to C_2- C_4 and give the lowest CH_4/C_2-C_4 ratio of all the catalysts tested. The amount of CO disappearing to C_5^+ is also modest as is the production of R-OH. Notably outstanding for the iron catalysts is the high olefin/paraffin ratio of the C_2-C_4 hydrocarbon. The iron catalysts generally give high CO_2 yields. This was expected since iron is known to be a good catalyst for the water gas shift reaction. Iron catalyst 22 prepared by precipitation of the nitrate and containing copper as a promoter was not active at 225° C. However, it became quite active at 265° C (Table III).

Catalysts 22 and 26 contain copper as a promoter, however, the activities and product distributions of these catalysts are comparable with iron alone on Kieselguhr (23) and sintered iron synthetic ammonium catalyst (ICI). The latter was very active and altogether gave the most favorable product distribution of all catalysts tested. The effect of copper on iron catalyst is not known at this time and is a subject for further work.

Table III gives further data on iron catalysts. Catalyst (ICI) was given two different reduction treatments. Pretreatment by reduction in H_2 at 550° C followed by nitriding with NH_3 at 325° C gives a catalyst which is more active than pretreatment with H_2 at 450° C (temperature required for similar conversion was 25° C higher than that for the same catalysts with pretreatment b). The important difference here is the step of nitriding in the pretreatment step. Such a step is known to make iron catalysts more active for Fischer-Tropsch synthesis (13,14).

Data in Table III for catalyst 22 shows the effect of temperature on catalyst activity. Whereas this particular iron catalyst was inactive at 225° C it becomes quite active above 265° C. Table IV shows the effect of on-stream time on catalyst 26. Activity appears to drop quite rapidly with time and after 10 hours was almost nil; however, raising the temperature to 250° C restored the catalyst to moderate activity. Treating the catalyst with H_2 at 450° C restores the catalyst to near its previous activity. The cause of activity loss while on stream and its restoration are not understood at present but this may have to do with blocking of the catalyst surface by high molecular substances which are produced in small amounts but which do not leave the catalyst surface at the temperature of reaction. This is the subject of further investigation.

Cobalt Catalyst

Catalyst 33 is a cobalt on γ-alumina catalyst prepared by coprecipitation of cobalt and aluminum nitrates with sodium carbonate. This catalyst had low activity compared with iron but could be brought up to appreciable activity by raising the temperature to 250° C. At this condition, this catalyst showed high methane and C_5^+ production with no alcohol formation. Still the activity for C_2-C_4 production was considerable and these products were better than 40% unsaturated. These results make cobalt an interesting metal for additional study.

Copper Catalyst

Catalyst 34 is copper supported on γ-alumina prepared in the same manner as the cobalt catalyst. Copper has low activity and the principle product is R-OH, mostly methanol. This was as expected and it was also expected that copper would show CO_2 formation since it is an important component of low temperature water gas shift catalysts (15). Even though water was there as a product, copper showed no CO_2 formation. This is an interesting finding and should be studied further.

Nickel Catalyst

Catalyst K6 is a γ-alumina supported nickel catalyst prepared by precipitation as with previous copper and cobalt catalysts. This particular catalyst formulation contained copper as well. It is well known that nickel is an excellent methanation catalyst. Consequently, we have not yet examined nickel by itself in our treating program. Copper was found to alter the catalytic properties of cobalt in a favorable way for our purposes so a corresponding catalyst of nickel-copper was investigated. The data in Table II show this catalyst to have low activity requiring 275° C to show 18% conversion of the CO. Carbon dioxide formation indicates strong water gas shift tendency. Copper does not appear to be present as copper metal since no alcohol was formed.

Cobalt-Thoria

This catalyst Kl was prepared by a method given in the literature (16). Cobalt and thorium as nitrates were coprecipitated with ammonium carbonate solution and to the resulting slurry Kieselguhr was added. This mixture was then dried and pelleted. It was found to be highly active and produced high yields of paraffins particularly CH_4 and C_5 -C_{30} long chain hydrocarbons. The C_2- C_4 hydrocarbons were mostly saturated. This was expected based on data in the literature (16).

Ruthenium Catalyst

A catalyst based on this metal has not yet been tested. Literature data indicate that such a catalyst is likely to yield CH_4 and C_5^+ high molecular weight paraffins. It will, however, be tested under our conditions and reported later.

CONCLUSIONS

Catalysts based on iron and cobalt appear to have the most potential for synthesizing C_2-C_4 hydrocarbons. Future work will be concentrated on improving the selectivity and stability of iron catalysts. Additional effort is also indicated for cobalt and possibly nickel to improve selectivity. Some work is also planned on the mechanism of CO_2 production.

The water gas shift appears to be an important reaction between CO feed and water produced in the reaction. Additional effort is indicated to determine the activity of our catalysts for this reaction, and the role this reaction plays in our synthesis. Other types of catalytic metals and different supports will also be investigated in future work.

REFERENCES

1. Storch, H., Golumbie, N., and Anderson, R. B., The Fischer-Tropsch and Related Synthesis, Wiley, N.Y., 1951.
2. Anderson, R. B., Catalysis, vol. 4 (P.H. Emmett, ed), Reinhold, N.Y., 1956, Ch. 1-4.
3. Pichler, H., Advan. Catal., 4, 271 (1952).
4. Rousseau, P. E., Chem. and Ind., pp. 1758-1966, Nov. 17 (1962).
5. Pichler, H., and Schulz, H., Chem. Ing. Tech. 42, 1162 (1970).
6. Vannice, M. A., J. Catal., 37, 449 (1975); 37, 462 (1975).
7. Dalla Betta, R. A., Piken, A. G., and Shelef, M., J. Catal. 35, 54 (1974); 40, 173 (1975).
8. Dry, M. E., Shingles, T., and Boshoff, L. J., J. Catal. 25, 99 (1972).
9. Dry, M. E., Shingles, T. and Botha, van. H., J. Catal. 17, 341 (1970); 17, 347, (1970).
10. Cohn, E. M., Catal., vol. 4 (P.H. Emmett, ed.) Reinhold, N.Y., 1956, Ch. 5.
11. Dosher, J. R., Chem. Eng. Prog. 72, No. 9, p. 15 (1976).
12. Greene, S. A., Moberg, M. L., and Wilson, E. M., Anal. Chem. 28, 1369 (1956).
13. Anderson, R. B., Advan. Catal., 3,380 (1957).
14. Aristoff, E. Paper Pres. at Catalysis Club of Philadelphia, Apr. 29 (1951).
15. Slack, A. V. and James, G. R. Ammonia, Part II., p. 1, Marcel-Dekker, Inc., N.Y. (1974).
16. Anderson, R. B., Hall, W. K., Krieg, A., and Seligman, B., Amer. Chem. Soc., J. 71, 183 (1949).

TABLE I

Composition and Treatment of Catalysts Studied

Wt-pct (f)	ICI	22	23	26	33	34	K6	K1
Fe_3O_4	1/ 94.0	2/ --	2/ --	2/ --	3/--	3/ --	4/ --	4/ --
Fe	--	79.3	52.2	59.4	--	--	--	--
Cu	--	19.7	--	29.3	--	18.4	12.8	--
Co	--	--	3.9	--	14.7	--	--	49.2
Ni	--	--	--	--	--	--	13.7	--
CaO	2.0	--	--	5.9	--	--	--	--
MgO	0.3	--	--	0.9	--	--	--	--
Al_2O_3	2.5	--	--	3.7	85.3	81.6	73.5	--
SiO_2	0.4	--	--	--	--	--	--	--
K_2O	0.8	1.0	1.0	0.8	--	--	--	--
Kieselguhr	--	--	42.9	--	--	--	--	43.1
ThO_2	--	--	--	--	--	--	--	7.7

1/ Pretreatment a, e, b
2/ Pretreatment a, e
3/ Pretreatment c
4/ Pretreatment d

a   Reduced in H_2 at 550° C for 20 hr; then nitrided in NH_3 for 6 hr
b   Reduced in H_2 at 450° C for 20 hr
c   Reduced in H_2 at 500° C for 4 h4.
d   Calcined in air at 520° C for 4 hr, then reduced in H_2 at 275° C for 4 hr
e   Regenerated in H_2 at 500° C for 20 hr
f   Compositions of catalysts are based on the calculated quantities of each
    metal salt taken for preparation.

TABLE II

Operating data on catalysts tested

Catalyst	Fe 23	Fe 22	Fe 26	Fe ICI	Co 33	Cu 34	toTho2 K1	CuNi K6
Pretreatment*	a	a	a	a	b	b	c	c
Temp, °C	225	225	260	225	250	275	225	275
Pressure, psig	750	750	750	750	750	750	120	750
Space velocity, cc/gm/sec	1.54	1.54	1.54	1.54	0.77	0.77	0.6	0.77
H_2/CO	1/1	1/1	1/1	2/1	2/1	2/1	7/3	7/3
CO conversion, %	57.6	0.9	94.7	89.4	16.96	11.57	84.0	18.3
Product selectivity, %								
CO_2	51.6	0.0	64.7	39.4	5.3	0.0	7.0	63.1
CH_4	15.8	25.9	8.3	11.7	34.0	11.6	32.0	24.4
C_2-C_4	18.7	51.6	17.5	24.8	27.4	5.3	12.0	9.7
C_5^+	10.3	22.5	8.7	22.0	33.3	1.2	49.0	2.8
R-OH	3.6	0.0	0.8	2.1	0.0	81.9	--	0.0
O/P	2.0	2.2	1.3	2.9	0.77	0.44	0.14	0.06

Pretreatment*
a Reduced in H_2 at 550° C for 20 hr nitrided in NH_3, 325° C for 6 hr
b Reduced in H_2 at 520° C for 4 hr
c Calcined in air 520° C for 2 hr reduced in H_2 at 275° C for 4 hr.

144

TABLE III

Effect of pretreatment and temperature of reaction for commercial
iron catalyst

	ICI-35-4		22		
Pretreatment	a	b	a	a	a
Temp, $^{\circ}$ C	225	250	225	265	250
Pressure, psig	750	750	750	750	750
Space velocity, cc/gm/sec	1.54	1.54	1.54	0.77	0.77
H_2/CO	2/1	1/1	1/1	1/1	1/1
CO conversion, %	89.4	75.9	0.9	47.7	20.7
Product selectivity,%					
CO_2	39.4	57.9	0.0	54.3	50.0
CH_4	11.7	2.5	25.9	8.5	8.1
C_2C_4	24.8	21.5	51.6	22.2	23.1
C_5^+	22.0	18.1	22.5	12.1	17.3
R-OH	2.1	0.0	0	2.9	1.5
O/P	2.90	4.65	2.2	1.62	1.5

a   Reduced in H_2 550° C, for 20 hr, nitrided in NH_3, 325° C for 6 hr

b   Reduced in H_2 at 450° C for 20 hr

TABLE IV

Effect of On-Stream Time and Regenerability of Iron Catalyst

Catalyst	Fresh 26*			21**	Regenerated with H_2 at 450° C for 20²hr	
Hr on stream	0.5	5.0	6.0	21**	0.5	4.0
Temp, °C	260	220	220	250	225	225
Pressure, psig	750	750	750	750	750	750
Space velocity, cc/gm/sec	1.54	1.54	1.54	1.54	1.54	0.77
H_2/CO	1/1	1/1	1/1	1/1	1/1	1/1
CO conversion, %	94.7	54.9	35.6	38.3	57.0	46.4
Product selectivity,%						
CO_2	64.7	46.0	45.3	39.3	52.8	44.8
CH_4	8.3	11.5	9.1	4.9	10.9	5.0
C_2C_4	17.5	19.0	18.4	15.7	17.7	20.7
C_5^+	8.7	22.3	25.9	31.8	18.6	29.3
R-OH	0.8	1.2	1.3	8.3	0.0	0.2
O/P	1.24	3.33	3.81	3.63	2.8	3.8

* Reduced in H_2 at 550° C 20 hr, nitrided in NH_3 for 6 hr (#26).

** Catalyst run discontinued at 10 hr left standing at 220° C in helium overnight; at hr 21 in the cycle the temperature was increased to 250° C
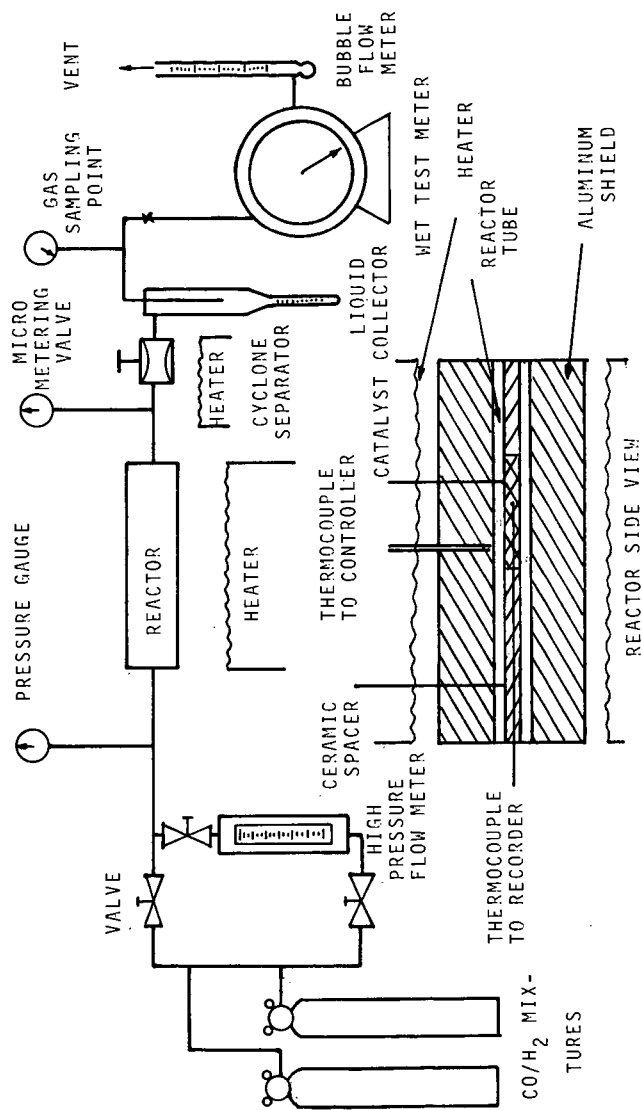
FIGURE I. - Reaction System Flow Diagram and Reactor Side View

147

"Studies on the Co-Cu-Al$_2$O$_3$ Catalyst System for
Conversion of CO and H$_2$ to Light Hydrocarbon Products"

Chen-Hsyong Yang, M. K. Zaman Khan, F. E. Massoth and A. G. Oblad

Department of Mining, Metallurgical and Fuels Engineering
University of Utah, Salt Lake City, Utah   84112

INTRODUCTION

Past research efforts on synthesis of hydrocarbons from CO and H$_2$ have been primarily devoted to two areas: synthesis of liquid hydrocarbons and production of methane (1). Early work was done mainly by Fischer, Tropsch and others in Germany. These researchers tested possible metal compounds in H$_2$/CO synthesis gas mixtures and they found that compounds of ruthenium, iron, nickel and cobalt were effective under various reaction conditions. They found that iron was the most effective catalyst for formation of liquid hydrocarbons when it was used under medium pressure reaction conditions (2). Recent methanation research showed that nickel was more selective for methane than cobalt, the latter producing more C$_2^+$ for the same conversion of CO (3).

Light hydrocarbons can also be produced in the Fischer-Tropsch process (4). CO and H$_2$ synthesis gas can be produced from coal with existing technology (5,6). By choosing an appropriate catalyst, CO and H$_2$ can then be used to produce light hydrocarbons as raw materials for the petrochemical industry.

In a previous paper, extensive studies of different catalysts for the conversion of CO and H$_2$ to light hydrocarbons were reported (7). Among others, a catalyst consisting of cobalt and copper supported on alumina was found to be promising for achieving the above-mentioned objective. In this paper, we report additional studies on this catalyst system. Work included catalyst characterization and testing of various catalyst formulations.

EXPERIMENTAL

The catalysts employed in this study were prepared by a co-precipitation technique. A hot solution of Na$_2$CO$_3$ was added to a hot solution of the nitrates of Co, Cu and Al dissolved in distilled water. The precipitate was filtered, washed and finally dried in an oven at 110°C. It was then ground to pass 200 mesh sieve, pelleted, reground and finally sieved, the fraction 14-25 mesh being retained for charges to the catalytic reactor.

In some formulations cupric chloride was used and in others (NH$_4$)$_2$CO$_3$ or NH$_4$OH was used in the preparation. In two of the latter preparations, Na was added to the oven-dried catalyst by impregnation. A listing of the catalysts is presented in Table I.

Catalyst analyses for Co and Cu were made by a spectrophotometic method. This consisted in dissolving the oven-dried catalyst in concentrated HCl and measuring the solution absorbance for Co at 690 mm and for Cu at 380 mm. Standard solutions were prepared for calibration purposes.

Characterization of a number of catalysts was carried out in a flow microbalance (8). These included measurement of degree of reduction and· O$_2$ adsorption on reduced catalysts. The following sequence was adopted for this purpose:

1) Heat in H$_2$ flow to 450°C.
2) Switch to N$_2$ and cool to room temperature.
3) Switch to air and measure weight gain.
4) Switch to H$_2$ and heat to 450°C.
5) Switch to air and measure weight gain.

All steps except 3) were run until weight was constant. In step 3), a rapid weight gain was obtained followed by a slow continued gain; this step was terminated after 1/2 hour. The amount of O$_2$ adsorbed was taken at the break in the curve in step 3).

The amount of reduced metal was calculated from the weight gain in step 5), assuming complete oxidation of the reduced metal was obtained. Overall weight loss in going from the oven-dried state to the reduced state via step 1) was consistently very close to 50% loss for the catalysts tested.

The above sequence was varied to study the effect of reduction temperature and the effect of a low temperature (250°) hold prior to heating to the higher temperature. Also, some adsorptions in step 3) were determined at 0°C instead of room temperature; no difference in initial adsorption was obtained, but the small continued weight gain was suppressed at 0°C.

X-ray analyses were performed on several reduced samples after O_2 chemisorption. Average particle size was estimated by line broadening using the strongest Cu line. Electron microprobe was used to examine Co and Cu distributions in the catalyst. This was accomplished by forming a tablet of the crushed material which after subjecting to reduction, was sliced at the midpoint and carbon-coated. Selected areas were probed for Co and Cu concentrations.

Catalyst activities were measured in a fixed bed reactor. Details are given in the previous paper (7). Catalyst pretreatments were made in-situ in the reactor. Reactor feed consisted of mixtures of H_2 and CO. Product gases were analyzed by gas chromatography for H_2, N_2, CO, CH_4, C_2-C_4 hydrocarbons, C_5^+ hydrocarbons and alcohols (predominantly CH_3OH). The C_5^+ fraction consisted of hydrocarbons from C_5 to C_{10} in decreasing amounts. Condensable liquid collected at room temperature was exclusively water, no measureable alcohols or hydrocarbons being detected.

CO conversion is defined as:

$$\text{CO Conversion} = \frac{CO_2 + \text{total hydrocarbons} + \text{alcohol}}{CO + CO_2 + \text{total hydrocarbons} + \text{alcohol}} \times 100$$

Hydrocarbon selectivities are defined as:

$$\%Y = \frac{Y}{\text{total hydrocarbons} + \text{alcohol}} \times 100$$

where Y represents C_1, C_2-C_4, C_5^+ or ROH. All values are calculated on a carbon atom basis.

RESULTS

Catalyst Characterization

One CoCu formulation was examined to determine pretreatment conditions appropriate for reduction to the metal and to estimate metal areas. The results are presented in Table II, together with data on a Co catalyst and a Cu catalyst. All tests were carried out starting with oven-dried catalysts. Heating to 450° in H_2 was sufficient to essentially completely reduce the Cu and the CoCu catalyst to the metals; but the Co catalyst was only about one-half reduced under these conditions. Under comparable reduction conditions, the CoCu catalyst showed about a ten-fold larger O_2 chemisorption compared with either the Co or Cu catalyst. On a per gram reduced metal basis, these results translate into a three-fold increase over the Co catalyst and a five-fold increase over the Cu catalyst in surface metal area. A two-stage heating schedule gave larger metal areas (greater O_2 adsorptions) compared to a direct heat up to maximum temperature. This was especially marked at 500°.

Reoxidation of the reduced samples caused changes in metal dispersion. Thus, reduction of the reoxidized CoCu catalyst gave a five-fold loss in metal dispersion. A lesser loss was obtained for the Cu catalyst and no loss was observed for the Co catalyst. Evidently, reoxidation of the reduced catalyst caused sintering of the highly dispersed metal phase. Pretreatment with N_2 in place of H_2 at 450°, followed by reduction resulted in a much lower metal dispersion, being only slightly greater than the reoxidized sample. Also, total reduction was somewhat lower (79%). Assuming all the Cu had reduced, this corresponds to about 50% reduction of the Co,

149

close to that obtained with the Co catalyst. Evidently, N_2 pretreatment is equivalent to air oxidation in causing metal sintering and Co interaction with the support.

X-ray analyses of reduced samples exposed to air showed Cu metal to be the major component, with Cu_2O as a minor component. The amount of Cu_2O relative to Cu was greater for those catalysts which had high O_2 adsorptions and negligible for low uptake catalysts. This indicates some surface oxidation of Cu occurred during exposure to air. The Co catalyst contained appreciable amounts of $CoAl_2O_4$ in addition to Co metal, accounting for its incomplete reduction. On the CoCu catalysts, a separate Co metal phase was not detected by x-ray analysis.

Estimates of average particle size from x-ray line broadening generally agreed with the O_2 adsorption results. Although average particle sizes based on adsorption did not give good quantitative agreement with the x-ray values as seen in Table II, the trends are nevertheless in the same direction. Uncertainties in the exact stoichiometry of adsorption and possible oxidation beyond the monolayer probably account for these differences.

Electron microprobe examination of the CoCu catalyst showed the distribution of Co and Cu across the pellet to be quite inhomogeneous, with some areas high and others low in concentrations of metals. However, in general, Co and Cu were located in the same vicinity.

Catalyst Activity

A complete product analysis for a typical run is presented in Table III. Hydrocarbon products were predominately normal straight chain molecules, small amounts of isomers only appearing at high conversions. Generally, olefin/paraffin ratios were low for C_2, about one for C_3 and low for C_4 compounds. The alcohol was exclusively methanol; small amounts of ethanol were only detected after prolonged reaction at high conversions.

Table IV shows the results of different pretreatments. The catalyst pretreated with H_2 at 520°C was more active for converting CO than the catalyst air calcined at 520°C, then reduced in hydrogen at 275°C. The catalyst that was held in hydrogen at 225°C for four hours, then at 520°C for another four hours was even more effective. However, hydrogen at high pressure with the two-stage temperature schedule during the pretreatment had an adverse effect on conversion of CO. Different pretreatment methods did not have much effect on hydrocarbon product selectivities.

Table V shows that increased sodium on catalysts caused a decrease in CO conversion; however, the relationship between sodium content and CO conversion was not linear. The two percent addition of sodium had the largest effect on CO conversion. The product selectivities were likewise affected, alcohol decreasing and the C_5^+ fraction increasing with sodium content.

Catalysts prepared with $CuCl_2$ were less active than those with $Cu(NO_3)_2$. Table VI compares two pairs of otherwise identical catalysts. In both cases, the catalysts prepared from the chloride had lower conversions, and lower C_5^+ and ROH selectivities. However, they had higher CH_4 selectivities.

The effects of process variables on conversion were briefly studied with one catalyst formulation; the results are given in Table VII. Larger conversions were obtained at higher temperature and H_2/CO ratio, while pressure had little effect. Selectivity-wise, the following trends were observed: (1) increase in temperature-higher C_2-C_4 and C_5^+ and lower CH_4 and olefin/paraffin ratio; (2) increase in H_2/CO ratio - lower olefin/paraffin ratio; (3) increase in pressure - no effect.

The effect of catalyst composition was studied in some detail. Figures 1 and 2 give conversions and selectivities for one run condition. Other run conditions gave similar trends. Conversion was found to correlate best with total metal loading. Conversion reached a maximum at a total loading around 18%. Thereafter, conversion levelled off or decreased slightly with increasing metal content. Production of CO_2 appeared to be closely related to CO conversion. Hydrocarbon selectivities correlated best with metal ratio. At one extreme, the Co catalyst

150

produced a high percentage of CH_4 and no ROH. As the fraction of Cu increased, CH_4 decreased and ROH increased. Of significance, C_2-C_4 was higher over a wide range of catalyst compositions. The C_5^+ fraction showed a similar trend. At the other extreme, the Cu catalyst gave high ROH with only a small percentage of CH_4 and C_2-C_4.

DISCUSSION

Catalyst Characterization

It is evident that Co and Cu interact during the prereduction step. The presence of Cu engendered reduction of the Co. The two together resulted in a much greater metal dispersion than each one separately. Sinfelt, (9) found a similar effect for RuCu and OsCu catalysts. Reoxidation caused appreciable sintering of the highly dispersed metals. Hence, air regeneration of aged catalysts would most likely cause a severe deactivation of the original catalyst activity.

The degree of dispersion was greatly affected by the pretreatment used. Oxidized and N_2 treated catalysts gave low metal dispersions after high temperature reduction, whereas direct treatment of the oven-dried catalysts with H_2 during heating gave much better dispersions. In the latter case, the heating schedule was important, viz., holding at 250° before subsequent high temperature heat-up resulted in even higher dispersions. Similar improvement in metal dispersion was found for Ni catalysts (10). Evidently, slow heating results in formation of small metals crystallites which are then stable at the higher temperatures. Increased metal dispersions were reflected in higher catalyst activities for CO conversion.

The increased dispersion found in H_2 pretreatment may be due to formation of an alloy phase or stable surface bimetallic clusters (11). The x-ray and electron microprobe results are in accord with this viewpoint. These states may be more stable towards sintering than crystallites of the individual metals. Further research along these lines is in progress and will be reported at a later date.

Catalyst Reactivity

Temperature had the most profound effect on catalyst activity and reaction path. Thus, at 250° and below, conversions were low and the major products were hydrocarbons and water; whereas at 275° and higher, conversions were high with formation of hydrocarbons and carbon dioxide. This is more or less typical of cobalt-containing Fischer-Tropsch catalysts (12).

At a given set of conditions, catalyst conversions increased with metal loading, as expected. However, the increase was not linear indicating that the amount of active metal surface area was not entirely proportional to the total metal present. Differences could reside in variations in degree of reduction and metal dispersion achieved for the various loadings. This is especially evident at the higher loadings, where conversions were found to tail off. The latter effect may be due to sintering of the basic metal crystallites to larger-sized particles.

The addition of copper as a promoter in Fischer-Tropsch catalysts was reported to facilitate reduction of the metal components, but not alter activity or selectivity (12). In addition to improving the reduction of Co, our CoCu catalysts also gave differences in selectivities. Thus, the Co catalyst gave selectivities relatively high in CH_4, low in C_5^+ and no ROH; whereas the Cu catalyst gave predominately ROH (Figure 2). In contrast, the CoCu catalysts gave moderate selectivities for CH_4 and C_5^+ and low ROH. The significant selectivity improvement with the CoCu catalyst was in the C_2-C_4 range, which approached close to 50% of the hydrocarbon product. Although product selectivities changed somewhat with increase in Cu to Co ratio, the C_2-C_4 selectivity was relatively insensitive to this parameter. The major effect was to decrease the C_5^+ and increase the ROH selectivities.

The addition of sodium to the catalyst had a depressing effect upon conversion. In addition, the C_5^+ selectivity increased while the ROH decreased. Sodium

addition to a Co:Cu (9:1) catalyst was reported to be unfavorable (13), resulting in increased molecular weight of products and rapid catalyst decline. Since most of the catalysts were prepared using sodium carbonate as the precipitant, some sodium may have been retained by the catalysts after washing. Comparison of conversions (Figure 1) indicates that up to 1% Na may have been present in the normally prepared catalysts. It appears that the sodium-free catalyst is somewhat more active.

The use of $CuCl_2$ in place of $Cu(NO_3)_2$ in the preparation had an interesting effect on catalyst performance. A decrease in conversion was accompanied by a decrease in ROH selectivity, strangely parallel to the effect of added sodium. The reason for this effect is not known at present.

ACKNOWLEDGEMENTS

REFERENCES

(1)   Anderson, R. B., Catalysis, Vol. 4, (P. H. Emmett, ed.), Reinhold, N. Y., 1956, Chap. 2.
(2)   Storch, H., Golumbie, N. and Anderson, R. B., The Fischer-Tropsch and Related Synthesis, Wiley, N. Y., 1951.
(3)   Mills, G. A., Steffgen, F. W., Catal. Review, 8, 159 (1973).
(4)   Rousseau, P. E., "Organic Chemicals and the Fischer-Tropsch Synthesis in South Africa", Chemistry and Industry, pp. 1758-1966 (Nov. 17, 1962).
(5)   Hoagendoorn, J. C., Gas from Coal with Lurgi Gasification at Sasol "Clean Fuels from Coal, IGT Symposium", pp. 111-126, September, 1973.
(6)   Farnsworth, J. F., Nitsok, D. M., Leonard, H. F. and Wintrell, R., Production of Gas from Coal by the Koppers-Totzek Process, "Clean Fuels from Coal, IGT Symposium", pp. 143-162, September, 1973.
(7)   Previous paper.
(8)   Massoth, F. E., Chem. Tech., 1972, 285 (1972).
(9)   Sinfelt, J. H., Catal. Review, 3, 175 (1970).
(10) Bartholomew, C. H. and Farrauto, R. J., "Chemistry of Ni/Al_2O_3 Catalysts", presented at the 68th Annual AIChE Meeting, November 16-20, 1975, Los Angeles.
(11) Sinfelt, J. H., AIChE. J. 19, 673 (1973).
(12) Anderson, R. B., Catalysis Vol. 4 (Emmett, P. H. ed.) Reinhold, N. Y. 1956, Chap. 3.
(13) Pichler, H., Adv. Catalysis, 4, 271 (1952).

Table I. Catalyst Compositions

No.[a]	wt., %[b]		Remarks[c]
	Co	Cu	
2	0	0	Al_2O_3 only
3	8.5	0	
4	0	13.0	
5	7.8	11.0	
7	7.1	8.8	
10	5.1	4.0	$(NH_4)_2CO_3$ used
17	7.5	4.9	
18	8.1	16.1	
19	7.4	1.3	
33	7.3	0	
34	0	12.3	
37	9.8	8.1	
38	6.4	8.8	
42	5.5	15.5	
43	5.0	3.4	NH_4OH used
44	4.8	3.6	NH_4OH used, 2% Na_2O added[d]
51	5.6	3.9	NH_4OH used, 1% Na_2O added[d]

[a]Catalysts above dotted line prepared with $CuCl_2$ and those below with $Cu(NO_3)_2$.
[b]Oven-dried basis
[c]Na_2CO_3 used for precipitation except where otherwise noted.
[d]Impregnation

153

Table II. Effect of Pretreatment on Metal Dispersions

Catalyst	Pretreatment[a] °C	Metal Reduced, %	Weight O_2 Chemisorbed,[b] mg/g	Av. Metal Particle Size, Å Adsorption[c]	Av. Metal Particle Size, Å XRD[d]
2	-/450	0	0		
3	250/450	46	1.5(1.5)[e]		
4	250/450	94	2.5(1.5)[e]	130(220)[e]	90(150)[e]
5	250/450	96	19.0(3.5)[e]	25(140)[e]	50(100)[e]
5	250/400	-	22.0	20	30
5	-/400	-	16.5	30	40
5	250/500	-	24.0	20	40
5	-/500	92	10.8	90	130
5	450[f]/450	79	4.5		

[a]H_2 used; 2h hold at each temperature.

[b]catalyst charge basis (oven-dried).

[c]based on ratio of weights of O_2 chemisorbed to redox change assuming one O per metal site.

[d]by x-ray diffraction line broadening.

[e]after high temperature oxidation-reduction cycle.

[f]N_2 used.

154

Table III. Analysis of Reaction Products

Component	Volume,%	Selectivity, %
H_2	55.3	
N_2	0.18	
CO	22.6	
CO_2	0.18	
CH_4	3.06	46.0
C_2H_4	0.021	
C_2H_6	0.135	
C_3H_6	0.157	28.4
C_3H_8	0.178	
C_4H_8	0.034	
C_4H_{10}	0.108	
C_5+	0.30	22.3
ROH	0.22	3.3
H_2O	0.40	

CO Conversion %   23.2

CO_2, %   2.7

Olefin/Paraffin   0.53

Catalyst 38, 18.47 g charge

Reaction conditions: 235°, 750 psig, $3H_2$/CO, 7.14 cc/sec

Table IV. Effect of Pretreatment on Conversion

Pretreatment[a]: Catalyst	CO Conversion, % A	B	C	D
7[b]	37	58		
38[c]		17	38	16

[a]Pretreatments:
  A - (1) air, 520°, 4 hr. (2) H_2, 275°, 2 hr., 5 psig.
  B - (1) H_2, 520°, 4 hr., 5 psig.
  C - (1) H_2, 225°, 4 hr. (2) H_2, 520°, 4 hr., 5 psig.
  D - (1) H_2, 225°, 4 hr. (2) H_2, 520°, 4 hr. 60 psig.

[b]Reaction conditions: 275°, 750 psig, $2H_2/CO$, 0.77 cc/g sec.

[c]Reaction conditions: 250°, 750 psig, $2H_2/CO$, 0.77 cc/g sec.

Table V. Effect of Sodium on Catalyst Activity

Catalyst	43	51	44
Na_2O, %	0	1	2
CO Conv., %[a]	22	19	2
Selectivity			
C_1	36	37	37
C_2-C_4	36	40	33
C_5^+	18	21	30
ROH	10.	2	0

[a]Reaction conditions: 275°, 500 psig, $2H_2/CO$, 0.77 cc/g sec.

Table VI. Effect of Copper Salt on Catalyst Activity

Pair	1		2	
Catalyst	10	43	7	38
Cu salt[a]	Cl	NO_3	Cl	NO_3
CO Conv., %[b]	9	39	59	90
Selectivity				
C_1	42	35	40	26
C_2-C_4	45	38	41	42
C_5+	13	19	18	26
ROH	0.2	8	2	6

[a] Used in catalyst preparation

[b] Reaction Conditions: 275°, 750 psig, $2H_2/CO$, 0.77 cc/g sec

Table VII. Effect of Process Variables on Conversion

Values are CO Conv., %

Temp.,°C		235		250	
H_2/CO		3/1	1/1	3/1	1/1
Pres. psig	750	34	13	77	37
	1000	41	10	–	29

Catalyst 38, 0.38 cc/g sec

FIG. I

CATALYST CONVERSION VERSUS METAL LOADING - RUN I

CONDITIONS: 275°, 750 psig, $2H_2/CO$, 0.77 cc/gs

□ CO CONVERSION, %   ⊠ NO Na,   ■ 1% Na,   △ CO_2, %

TOTAL METAL LOADINGS %

CO CONV. %

CO_2 %

158
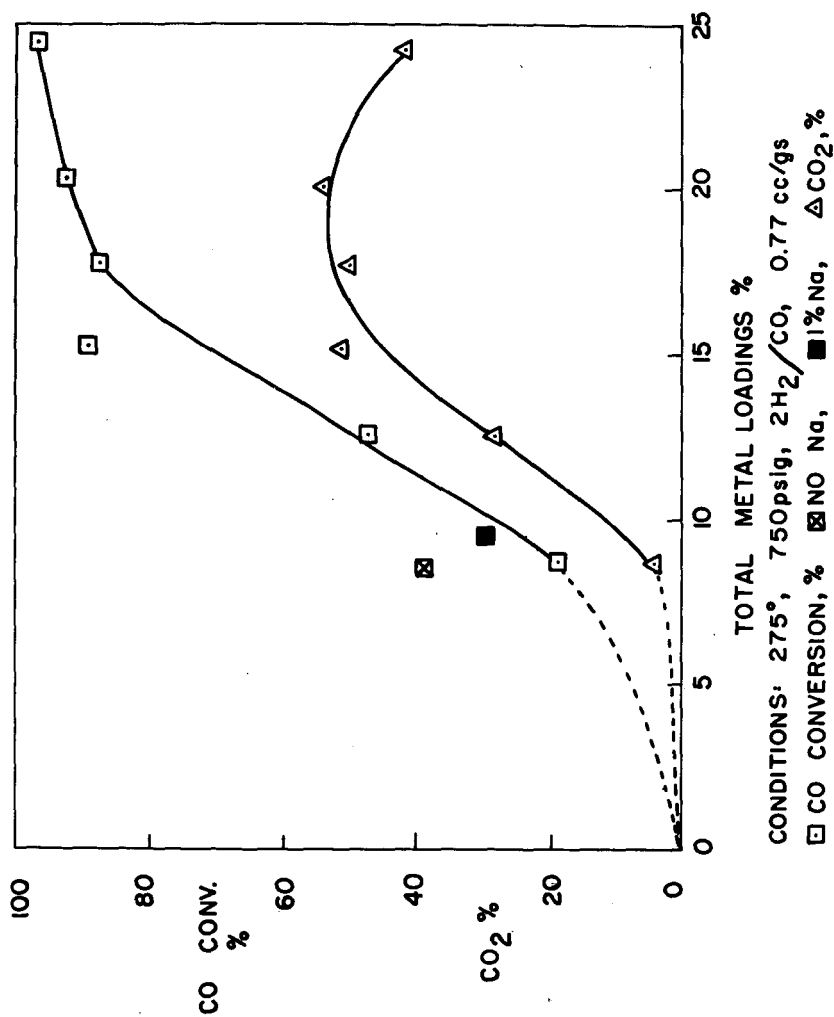
FIG. 2

CATALYST SELECTIVITIES VERSUS WEIGHT FRACTION COPPER - RUN I
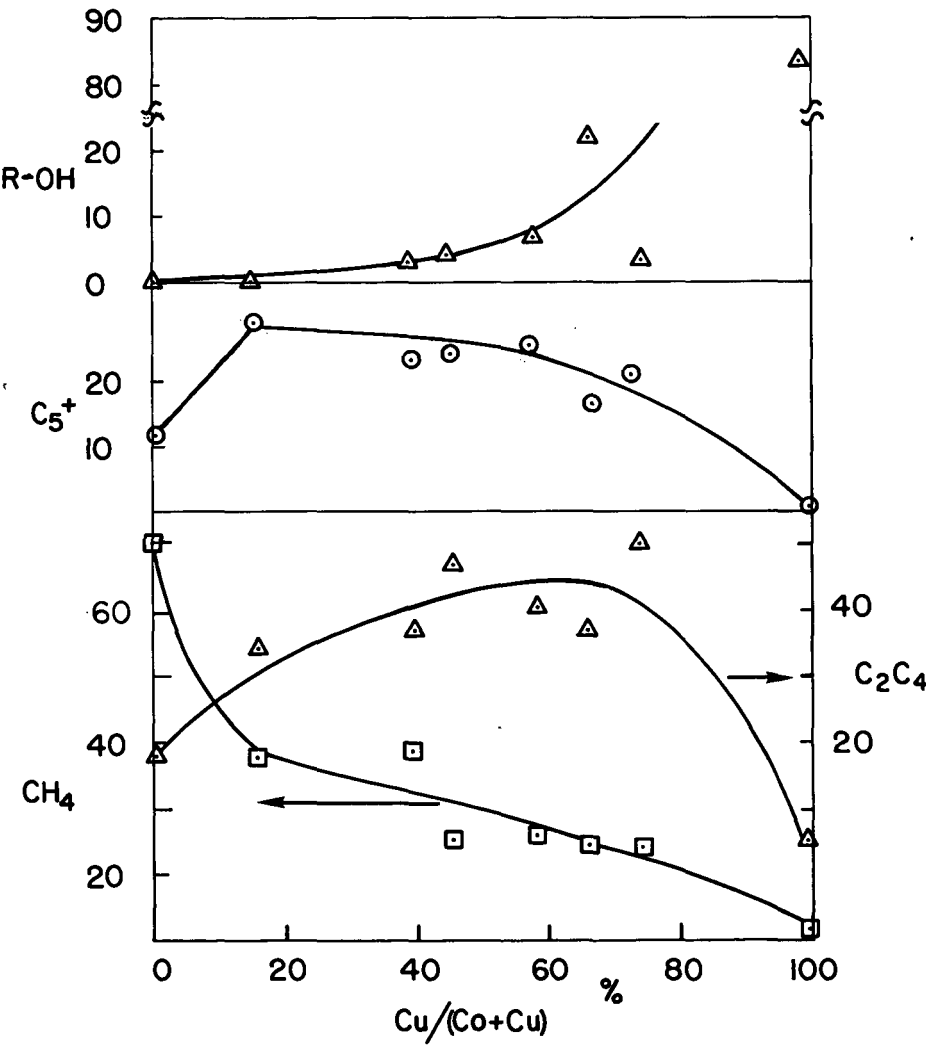
CONDITIONS: 275°, 750 psig, 2H$_2$/CO, 0.77 cc/gs

DONOR SOLVENT REACTIONS WITH COAL
IN A BATCH-RECYCLE SYSTEM

Doohee Kang, L. L. Anderson and W. H. Wiser

Department of Mining, Metallurgical and Fuels Engineering
University of Utah, Salt Lake City, Utah 84112

INTRODUCTION

Numerous reporst concerning kinetics of coal dissolution with hydrogen donor
solvent are available. However, little knowledge about the primary products
and the reactions which take place in experiments with short residence times
have been reported until recently.

This study involved the dissolution of coal in hydrogen donor solvent (tetralin)
in a rapid heat and rapid quench batch recycle system (Figure 1). The
residence time of the coal-solvent slurry was in the range of a few seconds
per pass in the slurry dissolver. The differential reactor system of batch
recycle applied here had two main advantages compared with conventional auto-
claves. 1) The rapid initial rate was expanded in the time scale of
differential conversions; consequently, the initial conditioning period was
minimized. In addition, continuous monitoring of data in a single run gave
more definitive and smoother results which could probably not have been
achieved by batch experiments. 2) A quench system was used which allowed
only a few seconds of thermal exposure of the slurry (at the reaction
temperature) per pass. This apparently reduced the reorganization and
polymerization reactions of the primary reaction products and permitted the
analysis of these primary fragmentation products from the dissolution process.

EXPERIMENTAL

A weighed amount of coal particles vehicled with small amounts of tetralin was
vacuum fed into the slurry mixer. When addition of coal to the system was
completed, hydrogen was used to purge and pressurize the system. Pumping of
the coal-solvent slurry was carried out at room temperature for about 10 - 30
minutes while the slurry mixer was stirred at 1200 rpm to achieve complete
suspension of the slurry throughout the system. The dissolver was heated to
the reaction temperature to start the experiment. Less than three minutes
was required to heat the slurry to 400°C in the dissolver. Flow velocity was
7.7 ft/sec when it was measured at the inlet to the preheater. Based on the
conditions of 400°C and 1500 psig H_2, about six seconds of residence time of
the slurry in the isothermal dissolver was achieved per pass. Slurry samples
were taken at the mixer in sizes to minimize system disturbance. Slurry
samples taken were weighed and centrifuged at 21,000 rpm for 40 minutes to
separate solid residue and liquids. Liquid portions of the samples are
subjected to gas chromatographic analysis to determine hydrogen transfer.
Other methods of analysis were applied to the extracts from the reaction such
as molecular weight and proton NMR.

Sequential washing of residual solids with fresh tetralin, benzene and pyridine was carried out to determine conversion data. Analysis of the ash content in the solid residues was used to determine the exact conversion figures. Gaseous products were collected in a liquid nitrogen double condenser in series at 77°K to trap the vapor products passing out through the gas vent. The rate of gas flow was kept to a minimum (approximately an average rate of 8 cc/sec at S.T.P.).

The following conditions were used for the system:

Temperature
slurry dissolver   400°C ± 5°C

quench outlet   50-70°C

Note: Too low a temperature at the quench outlet was avoided to prevent wall deposition of products which could occur even at high turbulence (7.7 ft sec).

slurry mixer temperature   100°C ± 2°C

Note: Low temperatures were avoided here for the same reason as above.

H_2
preheater inlet   1650 psig

dissolver   1500 psig

slurry mixer   1350 psig

Coal : solvent ratio = 1 : 9

Coal = Bituminous coal, Hiawatha, Utah
(V.M. =48.1%, F.C. =43.3%, ash =6.4%, S =0.7%)

particle size: 270/400 mesh, sp gr < 1.35

Figure 2 shows overall conversions data (pyridine soluble + gas, benzene soluble + gas and total gas) as a function of the residence time of the reaction. One set of numbers on the time scale (lower numbers) shows actual accumulated run time which is a time scale based on differential reaction. The upper numbers on the time scale represent the true residence time calculated as if reaction were carried out integrally. When coal particles are homogeneously suspended throughout the system, the relationship between these two time scale holds that,

$$t_i = \frac{w}{W} \, t_d$$

where t_i = residence time in integral conversion

t_d = residence time in differential conversion

w = mass hold up in dissolver

W = mass hold up in the remainder of the reactor system

Figure 3 shows net naphthalene and other tetralin derived compounds vs. percent conversion. Table 1 shows the gas composition from gas chromatographic analysis. Table 2 shows molecular weights of the products measured by vapor pressure osmometry.

As shown in Table 2 the average molecular weights of both the cyclohexane soluble portion and the tetralin soluble and cyclohexane insoluble portions gradually decreased as conversion proceeded.

DISCUSSION OF RESULTS

Figure 2 represents conversion-time data in real time and differential time. Figure 3 shows the same data in terms of naphthalene formation vs. conversion. Naphthalene formation was used here to indicate hydrogen transfer. From the data in both figures, two separate reaction regimes may be visualized. The kinetics are initially very rapid with minimal H_2 transfer. After about 1.5 minutes the conversion rate decreases and the transfer of hydrogen increases.

During the initial stages of the reaction, gas formation appears to predominate as shown by the gas production in Figure 2 and low H_2 transfer in Figure 3. The rate of gas production rapidly decreased after about 1 minute as shown by the nearly horizontal part of the curve in Figure 2.

Formation of gaseous products appeared to be concentrated in the first stage of the reaction. As can be seen in Figure 3 a negligible amount of hydrogen appears to have been transferred in the initial stages of the reaction. After the inflection point the following regime of reaction (after about 27% benzene sol. + gas) consisted of a slower overall reaction but one involving a rapid hydrogen transfer (up to around 60% of the benzene soluble fraction). Again there appeared to be a decrease in the rate of hydrogen transfer after about seven minutes of actual reaction time. These phenomena are strikingly similar to what Neavel (1) found except that inflections of the conversion curves were not observed in Neavel's experiments. This may point out one advantage of using the differential reaction system employed in our experiments. The fact that tetralin is consumed less than 20 parts per 100 parts of coal for benzene soluble conversion levels of around 80% shows considerable discrepancy from many previous results. (For example, some others have shown up to 40 parts of tetralin converted per 100 parts of coal.) Although our results cannot be directly compared for example to Neavel due to different experimental conditions such as a different tetralin:coal ratio (9:1 compared to 2:1) and a hydrogen atmosphere in our experiments, some of the same trends were observed.

The initial regime of the dissolution reaction appeared to be controlled by thermal disintegration of the coal with evolution of gases. The lack of tetralin penetration into the micro (internal) pore structure of the coal (which is known to comprise about 80% of the total pores of the coal) seems to make the solvent-coal reaction less important during the initial stages. Also coal is known to be bimodal with sizes of the internal pores distributed around 5Å to 8Å which would make it difficult for tetralin molecules

(diameter about 10Å) to enter these pores and make contact with internal reaction sites. Therefore, mere wetting of the external surface of coal may have taken place until opening of the micropores occurred by escaping trapped gases. An excess amount of solvent was supplied for the reaction (9:1 ratio of solvent to coal) since previous experiments by our laboratory and others showed that below approximately a 6:1 ratio of tetralin:coal the tetralin became the limiting reactant (2). Following the initial period of rapid donation of hydrogen from tetralin additional reaction paths may have been followed by introduction of tetralin into fresh reaction sites without restriction of diffusion into or out of the pores in the coal particles. The last stage of hydrogen donation appears to be controlled by diffusion either of fresh tetralin into the coal particles or products out of the particles. Even though the conversion rate is approximately constant (Figure 2) the hydrogen transfer rate after the initial rapid reaction is much less than the conversion rate as shown in Figure 3.

The data after about 10 minutes of actual reaction time for pyridine soluble and benzene soluble conversion were approximately the same. This is somewhat surprising since the initial reactions gave much higher benzene soluble yields. With the reaction system used the coal solvent mixture reached high temperatures followed by a quench which lowered the temperature to near ambient except during the time when the coal solvent mixture was in the reactor or heater. This gives some indication that perhaps this method of coal solvent interaction could improve product quality substantially.

The analysis of the gases which were released during the dissolution process which showed that methane formation was very small compared with that for other gases. This may or may not have implications as far as the linkages in the coal structure is concerned. As the carbon number of the molecules in the gas phase which appeared as products increased it is apparent from Table 1 that the fraction of the gases of a particular molecular weight which are normal straight chain hydrocarbon compounds decreased. This increasing ratio of unsaturates as the molecules became longer may be attributable to the longer lifetime of some free radicals which survive until the quench conditions change the temperature of the product mixture. As can be seen in Table 1 a substantial amount of isomers were formed for C4 compounds.

Substantial amounts of dihydronaphthalene were formed during the dissolution process. The formation of this dihydronaphthalene appears either to have been related to mild hydrogen transfer conditions or to have been an intermediate in the dehydrogenation of tetralin (or naphthalene formation). The majority of the dihydronaphthalenes were formed in a very short time in the initial stages of the reaction. The amount of these dihydronaphthalenes gradually decreased as conversion proceeded after giving a maximum at the first data point taken for the reaction at 400° (at about six seconds) as shown in Figure 3. In this tetralin excessive environment, dihydronaphthalene might follow the trends shown if it were an intermediate in a reaction path leading to naphthalene from tetralin. Such a consecutive reaction scheme would include the steps:

$$\text{Tetralin} \xrightarrow{k_1} \text{Dihydronaphthalene} \xrightarrow{k_2} \text{Naphthalene}$$
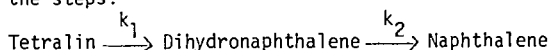
where the particular shape of the curves for dihydronaphthalene and naphthalene concentrations would depend on the relative values of k_1 and k_2 (assuming the reactions to be simple first order). The species resulting from the formation of dihydronaphthalene turned out to be over 99% of 1, 2-dihydronaphthalene. Hexa-, octa-, and decahydronaphthalene concentrations follow the same trends as given by Neavel (1) although he showed smaller quantities formed. This is probably to be expected since his conditions and coal/solvent ratio were different. The formation of cis-decalin always prevailed over trans-decalin. The results concerning dihydronaphthalenes and decalins needs mechanistic explanation and further experimental work will probably have to be done to explain the results obtained. Especially important is precise analyses of all of the chemical species present as a function of reaction time (or extent of reaction).

REFERENCE

1. R. C. Neavel, "Liquefaction of Coal in Hydrogen Donor and Non-Donor Vehicles", FUEL, Vol. 55, July, 1976.

2. W. H. Wiser and G. R. Hill, A Kinetic Study of the Thermal Dissolution of High-Volatile Bituminous Coal, Symposium of Science and Technology of Coal, Ottawa, Canada, 1967, p. 162-167.

Table 1. Gaseous Compounds
(collected in liquid nitrogen at 77°K (-196°C))

From reaction of tetralin with Hiawatha Coal at 400°C
(Tetralin:coal = 9:1; weight basis)

Compound	%	% Composition in each Homologs	Composition sat/unsat.	% Composition of Homologs
C_1	.3	100	100/0	.3
C_2	32.6	82	82/18	39.7
$C_2 =$	7.1	18		
C_3	25.0	69	69/31	36.2
$C_3 =$	11.2	31		
iC_4	1.7	14*	60/40	12.1
C_4	5.6	46		
$1\&iC_4 =$	.9	7*		
$t,C2C_4 =$	3.9	33		
n,iC_5	3.5	56**	56/44	6.2
$allC_5 =$	2.8	44		
$allC_6$	5.1			5.1
$allC_7$	.6			.6
$allC_8$	.3			.3

* substantial amount of isomers

**mostly normal with small amount isomer on shoulder

Notes:

1. % Composition based on gaseous products up to C_8 vapors collected.

2. Gas chromatographic analysis with the following conditions:
   20 ft. activated alumina (F-1)
   program temperatures from 60°C to 280°C (8°C/min.)
   He carrier gas flow rate = 30 me/min.

Table 2. Molecular Weight of Extraction Products
from Coal Extraction with Tetralin at 400°C

Conversion (benzene soluble)	Cyclohexane soluble	Cyclohexane insoluble Tetralin soluble
11.5	669	1506
27.7	539	15010
31.4	794	1368
42.5	504	1288
58.6	430	1126
77.5	436	1203
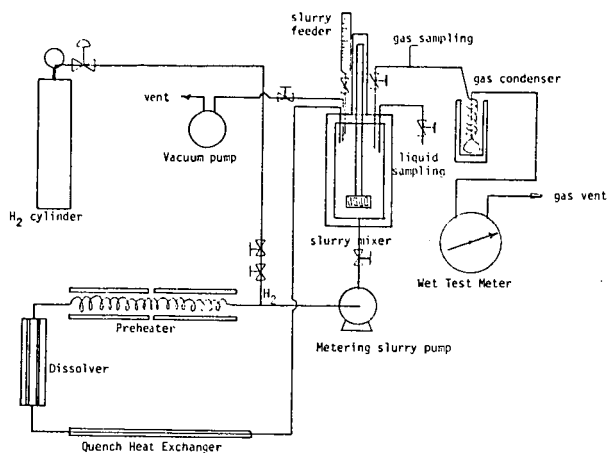
Figure 1. Batch recycle system for dissolution of coal in a hydrogen donor solvent.

Figure 2. Conversion data for Dissolution of Hiawatha (Utah) Coal at 400°C upper time scale is true reaction time; lower numbers are actual run time.

167
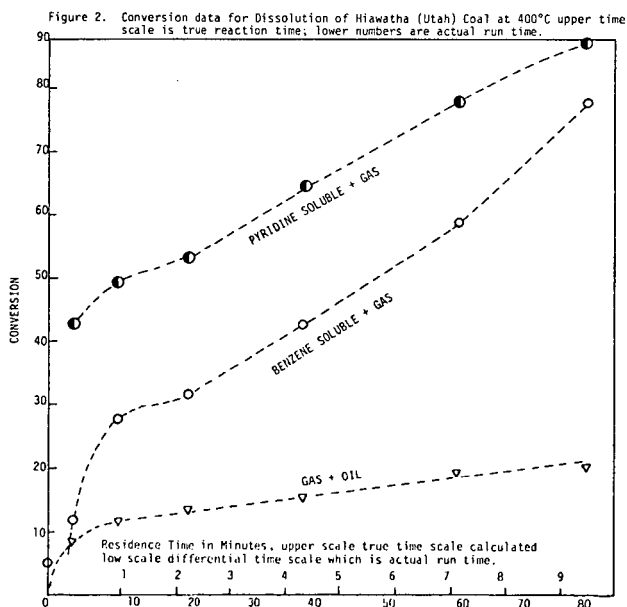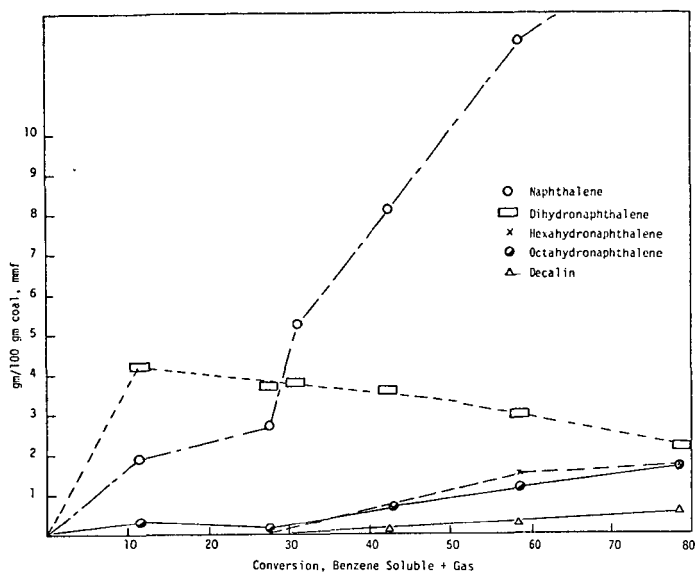
Figure 3. Hydrogen transfer as measured by tetralin derivatives from reactions with coal at 400°C (Hiawatha Coal)
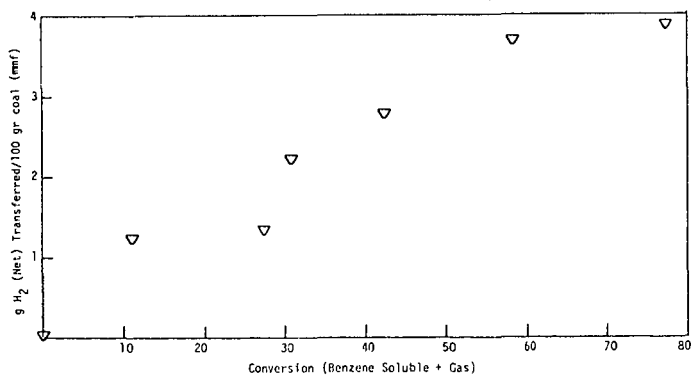
Figure 4. Net Hydrogen Transfer from Tetralin at 400°C in Reactions with Hiawatha Coal.

COMPOSITION OF SELECTED FRACTIONS FROM COAL TARS
PRODUCED FROM AN UNDERGROUND COAL GASIFICATION TEST

S. Bruce King

Energy Research and Development Administration
Laramie Energy Research Center
P. O. Box 3395, University Station
Laramie, Wyoming 82071

INTRODUCTION

The remaining fossil energy resources contained within the United States
are comprised primarily of coal. These resources have been estimated at 3.9
trillion short tons (1) or enough coal to provide this country with all of
its energy needs for the next two hundred years. One drawback with this vast
potential is the difficulty in utilizing this resource. Estimates indicate
that only 10-25 percent (1) is recoverable using present day techniques. The
remaining coal seams are either too deep or too low in quality to mine
economically.

In an effort to develop this inaccessable resource ERDA has sponsored
several different research programs in underground coal gasification. The
Laramie Energy Research Center has been developing a technique called the
linked vertical well (LVW) process to produce a low-Btu gas by gasifying a
coal seam in situ.

The field tests conducted at Hanna, (2,3) Wyoming, have shown that a
low-Btu gas can be produced and a great deal of control can be achieved in
directing the underground reaction systems, thereby resulting in high
utilization of the coal. The most recent field test conducted from April
through July of 1976 showed a total of 6700 tons of coal utilized and pro-
duction rates up to 12 MM scf/day. (4) The highest heating value obtained
for a substantial period was approximately 175 Btu/scf. In addition to this
low-Btu gas an organic condensate was co-produced with the gas. For lack of
a better term, this organic liquid has been called a coal tar. Its compo-
sition has been studied for various reasons, one of which is to ascertain
its value as a petrochemical feedstock or fuel.

Another consideration is the possible changes in composition due to
changes in reaction conditions. Additionally, the possible environmental
effects of such a by-product on groundwater quality must also be accounted
for since the seam is considered to be a low-grade aquifer. With these
thoughts in mind, the characterization was started to possibly answer these
questions.

DESCRIPTION OF THE LINKED VERTICAL WELL (LVW) PROCESS

The coal seam at the Hanna site is 30 feet thick, approximately 300 feet
deep and of subbituminous rank, a coal typical of most Western coals.

Numbers in parentheses refer to references at the end of the text.

The LVW process involves two distinct and separate steps. The first is a linkage step to achieve the desired permeability necessary for the subsequent gasification. This linkage is achieved through a reverse combustion process as shown in Figure 1 and then the gasification step using a forward combustion process follows. The produced gases flow through the previously formed linkage path to the production well and finally to the surface. The coal tars are produced within the reaction zone and carried to the surface with the produced gas.

The particular sample to be discussed in detail was produced during the first test at Hanna (collected on December 10, 1973) but reference to other samples from more recent tests will be made.

EXPERIMENTAL

Nonaqueous titration of nitrogen was performed in acetic anhydride and benzene with $HClO_4$ as described by Buell. (5) GLC analyses of tar acids were done on a 10' x .055" 10% SP-1200/1% H_3PO_4 on Chromosorb W AW column. With a helium carrier gas, a flow rate of 70 ml/min, isothermal for 2 min at 130° C, then 2° C/min increase to 200° C, a usable separation of components resulted. GLC analyses of the aliphatics were done on a 20' x .055" 3% SP-2100 on Supelcoport column. With a flow rate of helium carrier gas at 70 ml/min, isothermal at 50° C for 4 minutes, then a 2° C/min increase to 300° C, a usable separation was achieved. GC-MS data were collected on a system using a HP-5712 gas chromatograph interfaced to an AEI MS-12 mass spectrometer.

Simulated distillations were performed with use of gas chromatography with residue defined as any material that does not boil below 1000° F.

Fractionation into basic, acidic and neutral fractions was accomplished by aqueous mineral acid, sodium bicarbonate, and caustic soda extraction, pH adjustment to regenerate the species and extraction with diethyl ether. Neutrals were also separated into aliphatic and aromatic fractions with the use of silica gel. Hexane was used to elute the aliphatics and methanol to remove the aromatics.

PHYSICAL PROPERTIES

The following range of physical properties were determined from many samples collected during the three different tests conducted at Hanna, Wyoming.

Table I - Physical Properties

Specific gravity at 60° F	- 0.960 - 0.977
Viscosity at 100° F	- 3.5 - 13.2 centistokes
Heat of combustion	- 14,000 - 17,300 Btu/lb

As shown in Table I the physical parameters of these coal tars are desirable, in particular, they are very mobile compared to typical coal tars.

CHEMICAL PROPERTIES

The elemental analysis (Table II), for the sample collected on December 10, 1973, is typical for most of the tars produced from the underground coal gasification tests at Hanna.

Table II - Elemental Analysis

C	-	86.33 %
H	-	10.43
N	-	0.79
S	-	0.18
O^a	-	2.27

^{a}Percentage determined by difference

The maximum values for nitrogen and sulfur that have been observed are 1 percent and 0.5 percent respectively.

Another technique used for analysis is simulated distillations. The simulated distillation of the coal tar (collected December 10, 1973) is shown in Figure 2. The interesting point is the fact that none of the material boils above 950° F. When compared with the simulated distillation of a coal tar produced by laboratory carbonization (Figure 3), the obvious difference is in the boiling point distribution. With use of internal standard, it was determined that the carbonized laboratory sample was 24 percent (weight) residue or material boiling above 1000° F versus 0 percent for the UCG sample (Table III).

Table III - Boiling Range Distribution

Sample	Amb-400°F	400-500	500-600	600-700	700-800	800-900	900-1000	Residue
Carbonized	0	11.3	16.3	13.1	15.2	12.4	7.5	24.2
UCG sample	6.2	16.9	25.6	28.2	16.0	5.3	1.8	0

This demonstrates an important point about the UCG coal tar. It is a fractionated portion of the total produced coal tar. The passage through the production path up to the surface from the reaction zone acts as a preliminary separation step before presenting the coal tar at the production wellhead. This also explains the rather low viscosity of the tar since the more volatile components are produced at the surface. This provides a rather unique product for characterization when compared to typical coal tars.

Non-aqueous titration of the sample is shown in Table IV.

Table IV - Non-Aqueous Titration Results

Sample from December 10, 1973	0.524% WB	0.186% VWB

Strong, weak and very weak bases are defined by their half neutralization potential (HNP), with very strong bases having an HNP less than 150 mV, weak bases between 150 and 350 mV, and very weak bases greater than 350 mV. Pyridines and quinolines will titrate as weak bases and amides as very weak bases. Primary and secondary anilines titrate as very weak bases since they will acetylate and then titrate as amides.

The separation of numerous samples into tar bases, tar acids (strong and weak acids) and neutrals gave the following range of results (Table V).

Table V - Compositions Wt % of Tar

Tar Bases	2.5 - 8.0%
Tar Acids	.1 - 1 % - Strong Acids
	12 - 31% - Weak Acids
Neutrals	55 - 77% - 70% Aromatic
	30% Aliphatic

In addition, the neutrals were separated into aliphatic and aromatic fractions. The interesting point was that after looking at many samples, the relative amount of aliphatics vs. aromatics was essentially constant (30:70). Previous work (6) on the bases indicate them to be primarily quinolines with some pyridines and anilines, much as would be expected in a liquid product produced from coal.

The results presented in this paper are concerned with the composition of the weak acid and aliphatic fractions of this one sample as identified by GC-MS and NMR analysis. Although complete analyses have not been finished on other samples, a comparison of the weak acid and aliphatic fractions from other samples will be made.

The sample from December 10, 1973, was 14.5 percent (by weight) weak acids and 23 percent (by weight) aliphatics.

WEAK ACIDS

The composition of the weak acid fraction is almost exclusively phenolic in nature. With the use of GC-MS a reasonable separation (Figure 4) and subsequent analysis was obtained. Table VI lists the resulting components determined. In some cases the GC resolution was adequate enough to provide a mass spectra "clean" enough to identify specific isomers but in most cases only enough information was available to determine molecular weight and/or degree of alkylation.

Table VI - Weak Acids

phenol
p - cresol
o - cresol
m - cresol
4 different xylenols
7 C_3 - phenols
5 C_4 - phenols
small amount of aromatic aldehyde or ketone

Additional spectral information was obtained by manually trapping peaks eluted from the GLC and using H^1 and C^{13} NMR techniques to identify the components. Without the presentation of the data, the H^1 and C^{13} NMR spectral data support the conclusions of the GC-MS analysis.

ALIPHATICS

The aliphatic fraction showed very little in the way of unsaturation or cyclic compounds but a very high concentration of saturate components. The results (Table VII) show a normal hydrocarbon series going from C_{10} all the way to C_{32}.

Table VII - Composition of Aliphatics

1.   n-C_{10} through n-C_{32} series
2.   Branched Saturates { 2,11 - Dimethyl tridecane ($C_{15}H_{32}$) 2 - Methyl tetradecane ($C_{15}H_{32}$) 4,11 - Dimethyl pentadecane ($C_{17}H_{36}$) 6 - Methyl octadecane ($C_{19}H_{40}$) 7 - Methyl octadecane ($C_{19}H_{40}$) 3 - Methyl octadecane ($C_{19}H_{40}$) 3,6 - Dimethyl heptadecane ($C_{19}H_{40}$) two polybranched $C_{19}H_{40}$ 2,4 - Dimethyl octadecane ($C_{20}H_{42}$)

A small amount of branched saturates are also observed with a rather large concentration of C_{19} branched saturates. As seen in Figure 5, the GLC trace for this sample shows the distinct normal series with the branched C_{19} series at about 70 minutes retention time. No C^{13} or H^1 NMR spectra were run on this sample since the GC resolution was sufficient to provide reasonable GC-MS analysis.

COMPARISON OF SAMPLES

Although analysis by GC-MS and NMR of other weak acid and aliphatic samples are not complete and ready for presentation, the author feels that the following evidence of similarity between samples will be of interest.

The only data presented is the very noticeable resemblance between GLC traces for the weak acids and aliphatics from different samples (Figures 6, 7, 8 and 9). The coal tars represented by these fractions were collected during different tests at the Hanna, Wyoming site. The sample previously discussed was collected in the first test during December of 1973. The next tar (Figures 6 and 8) was produced in the second test operated from April til August of 1975. The third sample (Figures 7 and 9) was collected during the most recent test from April through July 1976. Simple observation of the three GLC traces (Figures 4, 6 and 8) for the weak acids show a very strong similarity, indicating a very similar composition for the three fractions. A corresponding similarity is noticed for the aliphatics (Figures 5, 7 and 9) except for the concentrations of what appears to be the n-C_{25} component in the 6-25-75 sample (Figure 7). Other than that one difference, which the author cannot provide an explanation for, the fractions all have a normal saturate series from about C_{10} to C_{31} or C_{32} and a C_{19} branched series at 70 minutes retention time.

Other samples have shown this same general character within all their fractions although they are not presented here. The overwhelming conclusion is that the coal tar is fairly constant in composition, not only during the life of an experiment, but also from one test to another as long as the tests are in the same coal seam.

This would appear to be a very desirable by-product of the gasification process due to its constancy. Additionally, the consistency of composition would indicate a process approaching steady-state conditions since there does not appear to be variation in one of its products, the coal tar.

EXPLANATION OF COAL TAR FORMATION

The following discussion is based not only on the composition of the coal tars but also on the other available information pertaining to UCG and in particular the work conducted at Hanna, Wyoming.

The air reacts exothermically with the coal and/or char to provide heat for the then hot gases CO_2 and H_2O to react with the char to form CO and H_2. The still relatively hot gases pass into or by fresh coal which is then devolatilized to produce the coal tars. These coal tars are then fractionated according to boiling point since they continue to cool as they flow with the product gas away from the combustion zone or heat source. The heavier components remain within the seam until they are eventually consumed or thermally cracked to lighter compounds. This fractionation is based on the temperature of the passage and the velocity of the gas stream since entrained droplets might also be carried to the surface.

This might also provide a very convenient method of disposing of these heavy molecular weight materials that would be hard to handle on the surface. It also helps to decrease the environmental effects on the ground water quality, if the more soluble products (the volatiles) are produced at the surface and the less water soluble (the heavy ends) remain behind and are eventually consumed. The actual fate of these organics in the ground water within the seam will be determined in a test to be conducted during the spring of 1977.

CONCLUSIONS

Analysis of the weak acid and aliphatic fractions of a coal tar produced from an underground coal gasification test reveal interesting results. The composition of the weak acids is much as would be expected, alkylated phenols. The aliphatics have a normal saturate series running from C_{10} to C_{32} with some branched saturates and a particularly heavy concentration of C_{19} branched saturates.

The most important point is the similarity of samples over the life of a system or from test to test. Referring to the three questions proposed earlier, this similarity or constancy would indicate the following:

1. As a fuel or petrochemical feedstock, a constant feedstock would be very desirable.

2. The unchanging composition suggests a system approaching steady-state conditions.

3. Environmental problems would be reduced if the effluent was constant in composition, thereby limiting the number of components to be monitored.

As a by-product, the coal tar appears to be advantageous which only increases the attraction of underground coal gasification as a commercial process.

REFERENCES

1. P. Averitt, "Coal Resources of the United States, January 1, 1974," U.S.G.S. Bulletin 1412.

2. L. A. Schrider, J. W. Jennings, C. F. Brandenburg and D. D. Fischer, "An Underground Coal Gasification Experiment, Hanna, Wyoming," 49th Annual Fall Meeting of the Society of Petroleum Engineers of AIME, SPE 4993, October 1974.

3. C. F. Brandenburg, R. P. Reed, R. M. Boyd, D. A. Northrop and J. W. Jennings, "Interpretation of Chemical and Physical Measurements from an In Situ Coal Gasification Experiment," 50th Annual Meeting of the Society of Petroleum Engineers of AIME, SPE 5654, September 1975.

4. D. D. Fischer, C. F. Brandenburg, S. B. King, R. M. Boyd and H. L. Hutchinson, "Status of the Linked Vertical Well Process in Underground Coal Gasification," presented at the 2nd Annual Symposium on Underground Coal Gasification, Morgantown, WV, August 1976.

5. B. E. Buell, Anal. Chem., 39, 756 (1967).

6. S. B. King, C. F. Brandenburg and W. J. Lanum, "Characterization of Nitrogen Compounds in Tar Produced from Underground Coal Gasification," presented at the Spring ACS meeting (Fuel Chemistry Division) in Philadelphia, PA, April 1975.

NOTE: Any reference to specific brand names does not imply endorsement by the Energy Research and Development Administration.
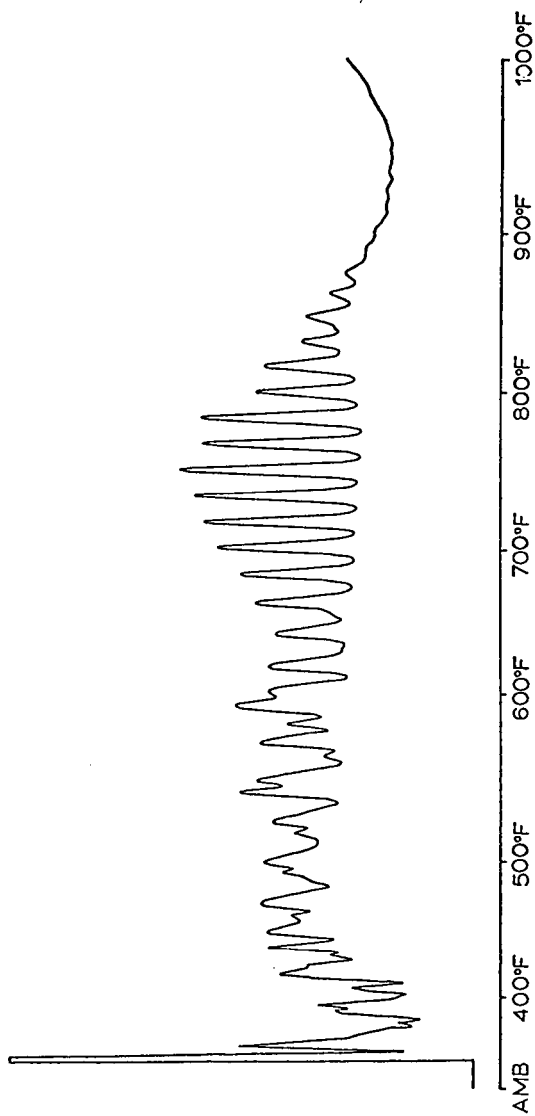
(A) VIRGIN COAL

(B) IGNITION OF COAL

(C) COMBUSTION LINKING FRONT PROCEEDS TO SOURCE OF AIR

(D) LINKAGE COMPLETE WHEN COMBUSTION ZONE REACHES INJECTION WELL (SYSTEM READY FOR GASIFICATION)

(E) COMBUSTION FRONT PROCEEDS IN THE SAME DIRECTION AS INJECTED AIR

(F) COMBUSTION FRONT EVENTUALLY REACHES PRODUCTION WELL
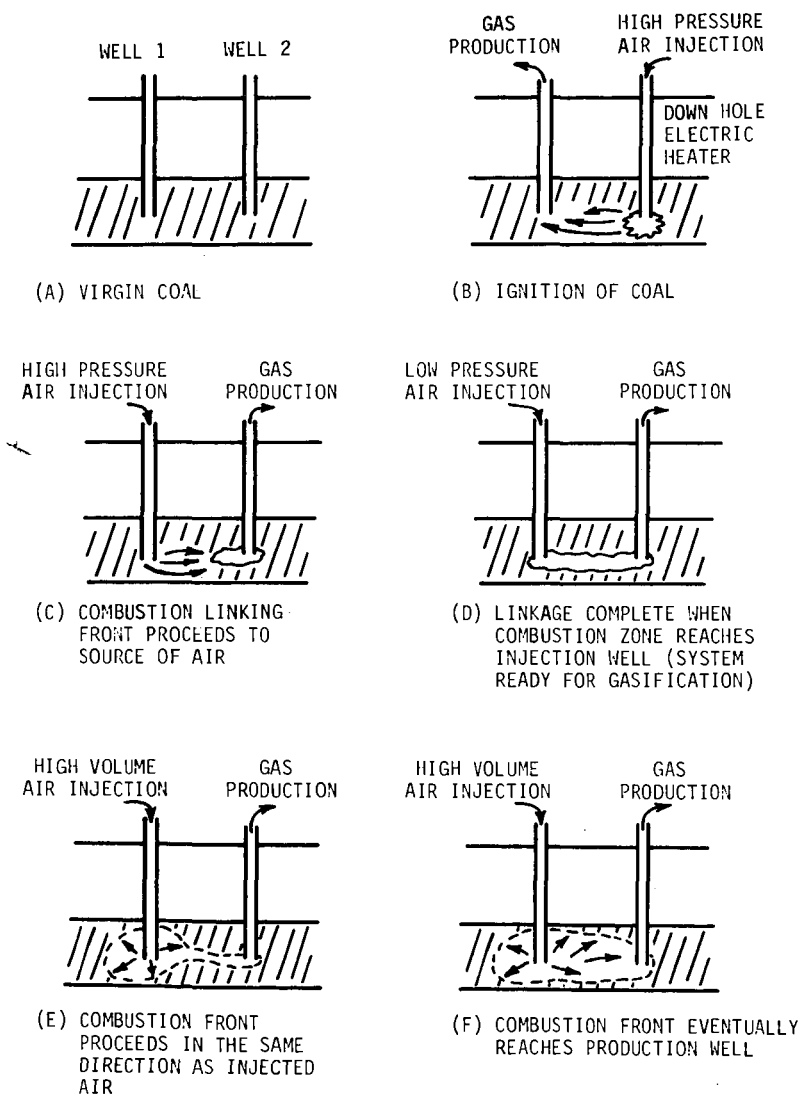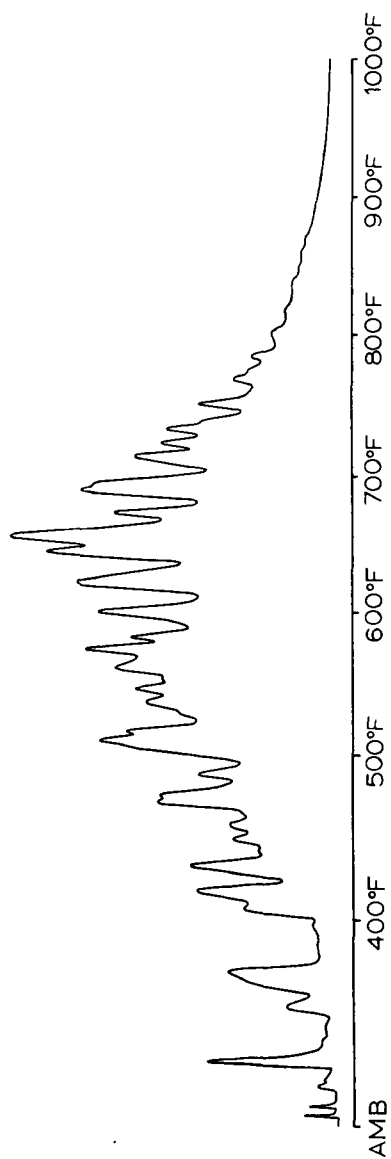
FIGURE 1

SIMULATED DISTILLATION OF TAR (12-10-73)

FIGURE 2

177

SIMULATED DISTILLATION OF COAL TAR
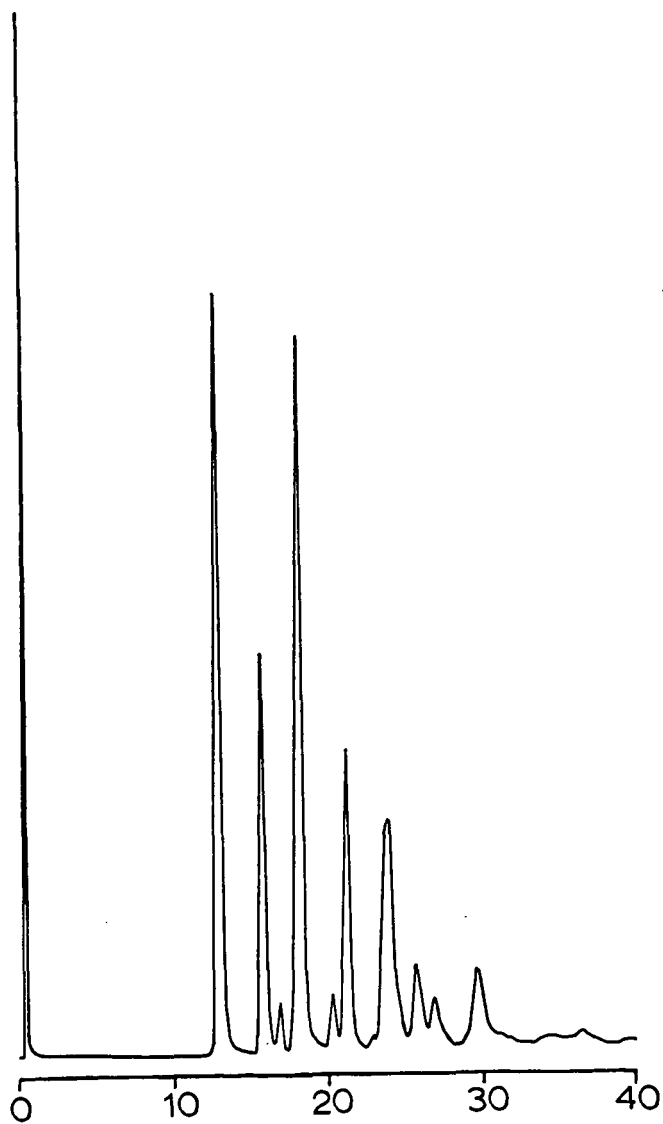PRODUCED BY CARBONIZATION AT 500°C

FIGURE 3
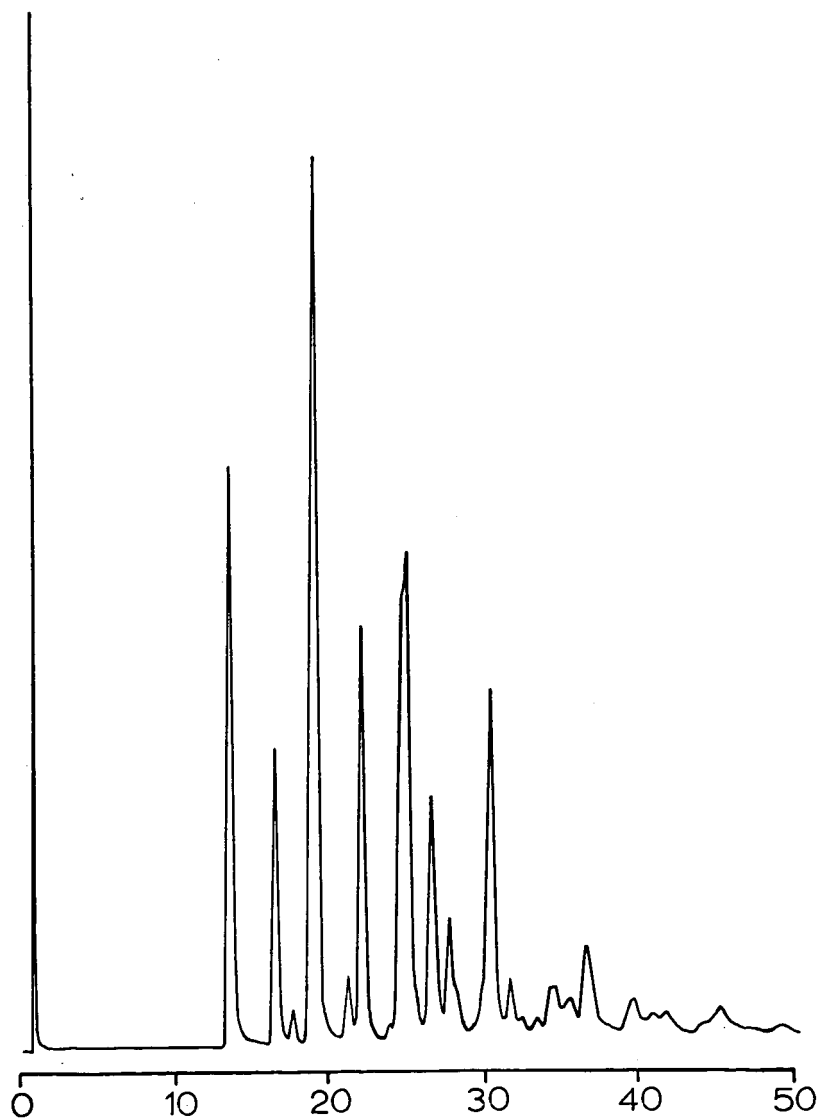
TAR ACIDS FROM (12-10-73)

FIGURE 4   179
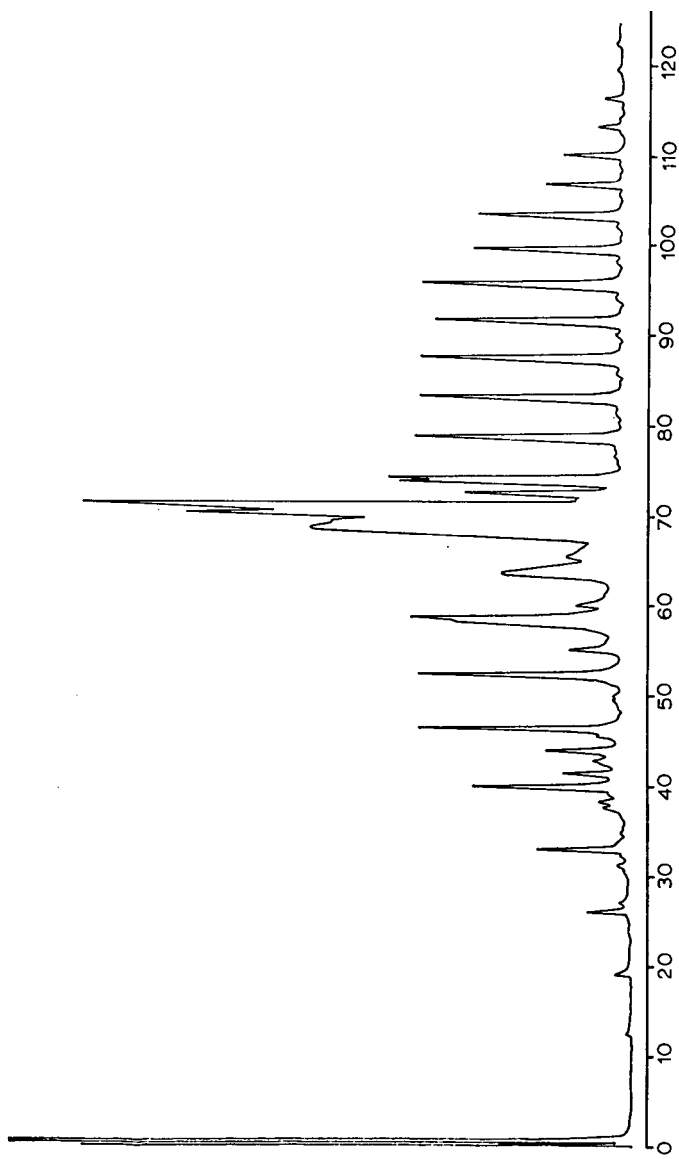
ALIPHATICS FROM (12-10-73)
FIGURE 5

TAR ACIDS FROM (5-21-76)

FIGURE 6   101
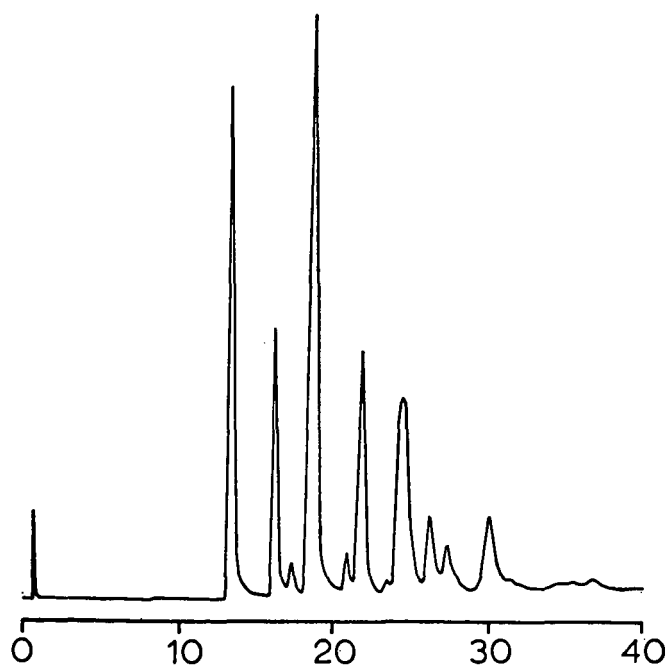
TAR ACIDS FROM (6-25-75)

FIGURE 7

182
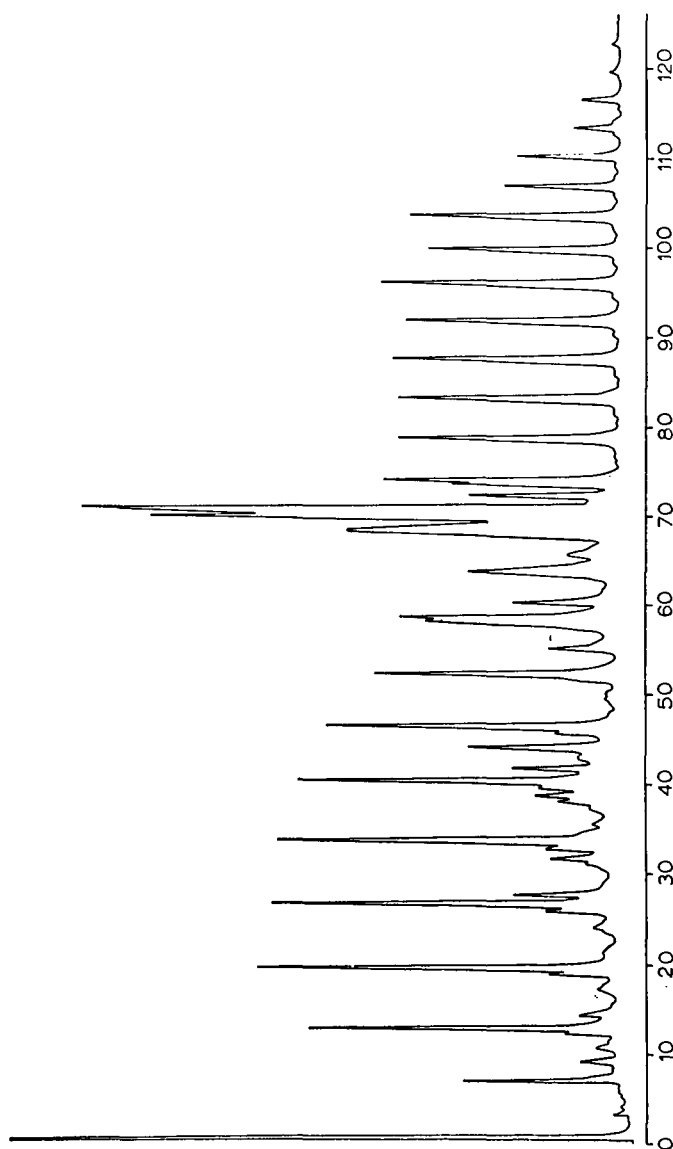
ALIPHATICS FROM (5-21-76)

FIGURE 8
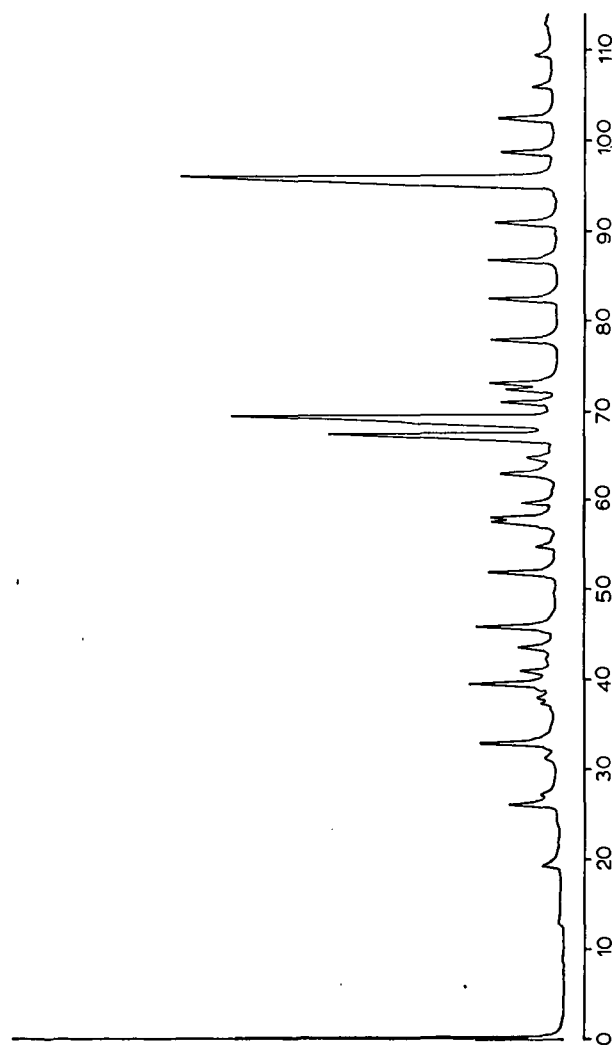
ALIPHATICS FROM (6-25-75)

FIGURE 9

184

COAL LIQUEFACTION UNDER HIGH-MASS FLUX AND SHORT-RESIDENCE
TIME CONDITIONS*

Carl L. Oberg, Arthur Y. Falk, George A. Hood, and James A. Gray

Rockwell International/Rocketdyne Division
6633 Canoga Avenue, Canoga Park, CA 91304

INTRODUCTION

This paper describes progress made during the first year of a program directed toward
developing and evaluating a concept for reacting pulverized coal with heated hydrogen
to form hydrocarbon liquids suitable for conversion to fuels or for use as chemical
feed stocks. The basic concept of the process is that high liquid yields are favored
by rapid mixing, reaction, and subsequent quenching of the reacting mixture. The
pulverized coal is being injected into the reactor by dense-phase transport, with a
minimum amount of carrier gas required. A rocket engine-type injector is being used
to rapidly and uniformly mix the coal with hydrogen that has been heated to 1200 to
2000 F. Reaction times of 10 to 1000 milliseconds at temperatures of 1500 to 1900 F
and pressures of 500 to 1500 psi are being explored. The concept is being evaluated
with a simple water-spray quench system.

The initial effort was directed toward cold-flow testing to develop suitable methods
of transport, injection, and mixing of the pulverized coal. Subsequently, reactor
testing was begun at a nominal coal flowrate of 0.2 tons per hour (tph). Prepara-
tions are also being made for testing at 1 tph.

COLD-FLOW TESTING

The purpose of the cold-flow testing was to develop effective means of feeding the
pulverized coal into a reactor and suitably mixing this coal with incoming hydrogen.
Dense-phase transport of the coal was chosen to minimize the gas requirement for
feeding the coal and, thus, maximize the gas available for heating, because the
process heat is supplied by heating the incoming hydrogen. Further, cold-flow mixing
tests were made to allow selection of injector configurations and operating conditions
that would produce a high level of mixing uniformity. This high mixing uniformity is
needed to ensure that the coal particles are exposed to a uniform reaction environ-
ment and reaction time during their brief residence time in the reactor. Poor mixing
would tend to cause some of the particles to be insufficiently reacted, thereby pro-
ducing a poor yield, and others to react for too long a period of time, with atten-
dant cracking of the oils into gases. This mixing optimization was accomplished by
adapting mixing characterization techniques that are used for performance optimiza-
tion of rocket engine injectors.

TRANSPORT AND FEEDING TESTS

Cold-flow tests were made with two simple pressurized feeders to evaluate the dense-
phase feeding and transport characteristics of the pulverized coal. One of these
feeders was made from a 4-inch-diameter Pyrex pipe 4 feet long and the second was
made from a 10-inch steel pipe 17 feet long. A 30-degree included-angle cone was
used in the bottom of each. Pulverized coal fed from each feeder through a ball valve
and through steel tubing into a catch vessel. No fluidizing gas was provided other

than that associated with pressuring the feeder. The transport gas requirement
was inferred from the rate of gas flow to the feeder during the flow of solids.
Pressures were measured at the top of the feeder and at several points in the feed
line.

Tests were made with two coal particle sizes--170 micron and 54 micron mass median
(27 and 74 percent through a 200-mesh screen). In most cases, nitrogen was used as
a carrier gas but tests were also made with helium and carbon dioxide to assess den-
sity effects. The coal was fed through 1/2-, 3/8-, and 1/4-inch tubing (inside
diameters of 0.402, 0.277, and 0.180 inch, respectively).

Typical pressure gradient results are shown in Fig. 1. An approximate minimum pres-
sure gradient is shown below which the coal would not flow. For each particle size,
the pressure gradient results tended to fall along a single line irrespective of tube
diameter. The coarser coal, which was used repeatedly because of a limited supply,
produced an increased pressure gradient with increased usage, although the results
still exhibited the same dependence on solids mass flux. The pressure gradient was
unaffected by the substitution of helium or carbon dioxide for nitrogen as the
transport gas. The difference in pressures between that measured in the feeder and
that measured near the upstream end of the feed line exhibited a similar dependence,
varying from 1.6 to 14 psi at solid mass fluxes of 400 and 1500 lbm/ft-sec,
respectively.

The transport gas requirement is shown in Fig. 2. The results indicate that the coal
is leaving the feeder at near its static bulk density and only the gas carried in the
interstices of the particles is required for transport.

The dispersed solids density was measured by simultaneously closing two ball valves in
the line to trap the amount of solids being carried. For the 170 micron coal, this
density exhibited a power law dependence on solids mass flux, varying from 50 to 30
lbm/ft^3 at 150 and 700 lbm/ft^2-sec for each carrier gas.

Results from this testing have shown that pulverized coal can be effectively fed
from a simple pressurized feeder. The dense-phase flow is smooth and reproducible.
Flowrates from ~0.1 to 1.0 lbm/sec were readily obtained. Flowrates ~10 lbm/sec
were obtained with another pressurized feeder, used for loading the 10-inch pipe
feeder.

COLD-FLOW MIXING TESTS

Cold-flow tests were also made to define coal/gas injector configurations and opera-
ting conditions which will give rapid and uniform mixing. Because techniques have
been developed for achieving and characterizing injector mixing for liquid-propellant
rocket engines, these techniques were adapted for the coal/gas case. Furthermore,
injector configurations known to give high levels of mixing in rocket engines were
considered primary candidates for the coal/gas case.

For this testing, nitrogen was chosen as a simulant for the heated hydrogen in the
reactor. Both the gas injection velocity and density were modeled in the cold-flow
case. The pressure in the cold-flow chamber was chosen to give a gas density corres-
ponding to that of the hydrogen at injection conditions. To model hydrogen at 1000
psia and 1500 F, the nitrogen pressure should be 19.1 psia. Consequently, the use
of nitrogen allowed the tests to be made at nearly atmosphere conditions.

A two-phase flow probe was used to characterize the flowfield created by the coal/
gas injection. Similar probes have been used extensively to characterize gas/liquid

injection for rocket injectors (e.g., Ref. 1 and 2). These probes have been developed from that originally used by Dussourd and Shapiro (Ref. 3).

The cold-flow mixing tests were made with a single injection element in the cold-flow chambers. A secondary flow of gas was also used in the chamber to suppress recirculation. Data from the probe tests were analyzed to calculate the local mass fluxes of a gas and coal. The local mass flux values were numerically integrated to obtain collection efficiencies by comparison with measured injection flowrates.

The resultant mass flux distributions were plotted for qualitative assessment; also, a mixing efficiency was calculated. The mixing efficiency used was one developed for rocket engine injector characterization by Rupe (Ref. 4). This mixing efficiency is usually expressed as

$$E_m = 1 - \sum_{r_i < R} MF_i \left(\frac{R-r_i}{R} \right) - \sum_{r_i > R} MF_i \left(\frac{R-r_i}{R-1} \right) \tag{1}$$

where $MF_i = \dfrac{(m_c + m_g)_i}{\sum (m_c + m_g)_i}$ and $R = \dfrac{\sum m_{ci}}{\sum (M_c + m_g)_i}$ and $r_i = \dfrac{m_{ci}}{m_{ci} + m_{gi}}$ and m_{ci}, m_{gi}

are the local mass flowrates of coal and gas, respectively, in the ith steamtube. A relatively simple interpretation of Eq. 1 can be obtained by recognizing that the terms in parenthesis in the equation represent local deficiencies of the fractional mass fluxes. The flowfield data were numerically integrated to obtain the mixing efficiencies.

Two coal/gas injector configurations were chosen for cold-flow evaluation: a concentric tube configuration and a 4-on-1 impinging configuration. Both of these yield high mixing efficiency in rocket applications. Further, they were not expected to result in substantial impingement of coal on the walls. The concentric tube element involves coaxial flow of the two streams with coal in the central tube and gas flowing in the annulus. The 4-on-1 element involves impingment of four gas streams on a central coal stream. The dimensions of the injection elements were also selected on the basis of rocket engine experience.

Results from the cold-flow mixing tests are summarized in Fig. 3 and 4. High levels of mixing efficiency have been obtained, with both types of elements. In rocket engines, mixing efficiencies greater than 80 to 90 percent lead to very high combustion efficiencies (>95 percent).

The mixing results obtained with the concetric tube element exhibit different trends from those obtained with gas/liquid injection element, probably because of differences in the shear interaction in the element. Conversely, the coal/gas 4-on-1 injector exhibits qualitatively similar characteristics to a gas/liquid or liquid/liquid injector. Optimum mixing was obtained with two different diameter ratios, although in each case, the mixing on only one side of the optimum has been defined.

These two results may be used to obtain a diameter ratio dependence as:

$$\left[(\rho u^2)_g / (\rho u^2)_c \right]_{optimum} = 12.6 \, (D_g/D_c)^{2.1} \tag{2}$$

or

$$\frac{D_g}{D_c} = \left[\frac{1}{12.6 \, (4^2)} \left(\frac{m_g}{m_c} \right)^2 \frac{\rho_{ds}}{\rho_g} \right]^{1/6.1} \tag{3}$$

187

High levels of mixing have been demonstrated with both the concentric-tube and 4-on-1 element configurations. The highest levels of mixing were obtained with the 4-on-1 configuration, although either type appears suitable on the basis of mixing for reactor testing. Furthermore, the ability to use a two-phase flow probe to characterize coal/gas mixing has been demonstrated.

REACTOR TESTING

Reactor testing currently under way is directed toward evaluation and development of a reactor based on the short-residence time concept. The reactors are being designed to promote rapid mixing (based on the cold-flow results) and to obtain relatively high gas velocities, to promote interaction (mass transfer and reaction) of the gas with the particle. The hydrogen is being partially heated by indirect heating and by partial combustion with oxygen as necessary to supply the required process heat. The reactor is being operated with high internal wall temperatures to minimize a tendency for adhesion of the partially reacted coal particles on the wall. The amount of hydrogen fed is being kept as low as practical because of the recycle implication for a complete process. A simple water-spray quench system is being used.

Reactor testing was begun with a system capable of feeding 35 lbm of coal at a planned flowrate of ~0.1 lbm/sec (~0.2 tph). The 0.2 tph reactor assembly is illustrated in Fig. 5 and a schematic flow diagram of the test system is shown in Fig. 6. The reaction chamber for most tests was a 1-1/2-inch-diameter, 0.049-inch-wall stainless steel (type 321) tube, 36 inches long. This reaction chamber is contained within an insulated pressure vessel made from 8-inch pipe. Coal is fed in dense phase to the reactor from a pressurized feeder of the type used during the cold-flow testing. The feeder is a 6-inch diameter vessel with a conical (15-degree half angle) exit. Reaction products pass from the reaction chamber into a quench section, which has a set of water spray nozzles, and into a char receiver. The hydrogen is heated in a 260-inch-long coiled tube that is heated by passing an electric current through the tube. Up to 150 killowatts of power is supplied to this tube by seven motor-generator sets. Nearly all of this power is transferred to the hydrogen as heat.

Two types of inejctors have been used: a concentric tube and a 4-on-1 configuration. The 4-on-1 injector configuration is shown in Fig. 7. The body of this injector is made from a 1-1/2-inch tube fitting tee. The heated hydrogen enters the injector from the side, flows around the insulated coal feed tube, and through four injection orifices. The four hydrogen streams impinge with a 30-degree half angle at a point 0.400-inch from the injector face. Also included are four oxygen injection orifices which also impinge with an angle of 30 degrees but at a distance of 0.700 inch from the injector face.

Initial testing was directed toward solving operational problems with the system. The initial tests were made with the concentric tube injector and without oxygen addition. The reactor temperature was found to be lower than anticipated during these tests. The reaction process appeared to exhibit thermally neutral character whereas exothermic character was anticipated. Hydrogen-to-coal flowrate ratios near 0.36 were required to obtain a reactor outlet temperature 1100 F. A reactor outlet temperature ~1500 to 1800 F was believed to be needed for high conversions. Further, it was found that the char in the reactor tended to agglomerate and adhere to the walls of the reactor. The latter problem was believed due to a low reactor wall temperature, which was ≤1000 F during initial tests. Feldmann et al. (Ref. 5) report that wall temperatures of 1340 to 1470 F were required in the Hydrane reactor to avoid wall adhesion. The system and operating procedures were modified to minimize heat losses from the reactor tube and, also electric wall heaters were tried. However, the wall temperatures were not increased sufficiently to eliminate the wall adhesion problem. Therefore, the system was modified to allow the addition of oxygen to raise the temperatures by partial combustion.

188

Two methods of oxygen addition were tried: (1) injection in a small combustor up-
stream from the injector, and (2) injection directly into the reactor. Relatively
small amounts of oxygen are required to increase the gas temperature to near 2000 F.
Both methods were successful, although some difficulties were encountered with over-
heating the injectors and preburners with the preburner approach. Agglomeration was
largely eliminated for reactor temperatures greater than ~1600 F and reactor plugging
due to wall adhesion did not occur with reactor temperatures above ~1500 F.

A series of tests was made to assess the effects of reactor temperature, location of
oxygen addition, residence time, and velocity.

The raw char gas samples, and aqueous samples from the tests have been analyzed to
determine the composition of the products and to allow calculation of material
balances. The gas samples were analyzed by gas chromatography for N_2, H_2, O_2, CO,
CO_2, and C_1 to C_4 hydrocarbons. A gas chromatographic analysis is used also for
benzene, toluene, and xylene. The latter procedure was confirmed by mass spectro-
metric analysis. Also, the sample bottles are washed with a solvent to remove tar-
like materials.

Aqueous samples from the cyclone and secondary separators and the water removed from
the char receiver have been analyzed for carbon content with a total carbon analyzer.

The raw char samples are weighed, air dried, and reweighed after which a portion of
the sample is dried in an oven at 221 F for 1 hour. A portion of the air-dried sam-
ple is sent to an outside laboratory for proximate and ultimate analyses. Also, an
analytical benzene extraction, employing a Soxhlet apparatus, is used to determine
an extractable fraction. Most of the extractions have been made with material dried
at 221 F for 1 hour. An ash analysis is also made.

Typical results from the 0.2 tph testing are shown in Tables 1 through 3, which sum-
marize the test conditions and product composition from four tests made with the
4-on-1 injector.

Carbon conversion results from the 0.2 tph testing are shown in Fig. 8, which shows
overall and gas conversions. Results are shown from tests made with a basic reactor
size of 1.402 inch diameter x 36 inch long and also with 0.995 inch diameter x 36
inch, 1.995 inch diameter x 36 inch and 1.402 diameter x 18 inch reactors. Thus,
the reactor residence time was increased and decreased by a factor of 2.0 from the
base case. The overall conversion has been calculated with the ash in the coal being
used as a tracer. In most cases the ash recovery was in the range of 90 to 100 per-
cent. The overall conversions appear to vary most strongly with temperature and
residence time, while changes in the location of oxygen addition (preburner or reactor)
and injector (concentric tube or 4-on-1) had relatively small effects. The effect
on conversion to gas of changing the location of oxygen addition was significant.
The increase in gas formed with oxygen addition in the reactor appears to result from
oxidation of liquid products.

Carbon conversion to liquids is shown in Fig. 9. Not all of the carbon was recovered
during many of the tests. This lost material is belived to be liquid, probably a
mist of small droplets not removed by the cyclone separator and settling tank. Some
tarry material was recovered from the gas sample bottles but the accuracy of that
sample is not sufficient for it to be used to account for the carbon deficit. Tar
quantities ranging from a few milligrams to a few grams have been obtained while
samples in the middle of this range would account for the loss. The carbon fraction
corresponding to the liquid obtained by benzene extraction of the char and tar re-
moved from the separators is shown in Fig. 9 along the fraction inferred by differ-
ence. The carbon deficit is shown in Fig. 10.

Current effort is directed toward improving the carbon recovery and preparation for reactor testing at 1 tph.

CONCLUSIONS

Results from the testing are regarded as highly significant and encouraging. Effective methods of feeding the coal and of injection and mixing of the hydrogen and coal have been developed. Significant progress has been made on developing the desired reactor process and feasibility has been demonstrated. For comparable flowrates, the size of this reactor is several orders of magnitude smaller than some of the other liquefaction reactors being developed.

The test results indicate high overall conversion, approaching that required for a balanced plant operation. Liquid yields also appear high, although the lack of total recovery leaves some uncertainty.

REFERENCES

1. Burick, R. J.: Space Storable Propellant Performance Program Coaxial Injector Characterization, Contract NAS3-12051, NASA CR-120936, Rocketdyne Division Rockwell International, Canoga Park, California, October 1972.

2. McHale, R. M.: Noncircular Orifice Holes and Advanced Fabrication Techniques for Liquid Rocket Injectors - Final Report Phases III and IV, R-9270, Rocketdyne Division, Rockwell International, Canoga Park, California, May 1974.

3. Dussourd, F. L. and A. H. Shapiro: "A Deceleration Probe for Measuring Stagnation Pressure and Velocity of a Particle Laden Gas Stream," Jet Propulsion, January 1958, pp. 24-34.

4. Rupe, H. J.: A Correlation Between the Dynamic Properties of a Pair of Impinging Streams and the Uniformity of Mixture-Ratio Distribution in the Resulting Spray, Progress Report No. 20-209, Jet Propulsion Laboratory, Pasadena, California, 28 March 1956.

5. Feldmann, H. F., J. A. Mima, and P. M. Yavorsky: "Pressurized Hydrogasification of Raw Coal in a Dilute-Phase Reactor," Coal Gasification, edited by L. G. Massey, Advances in Chemistry Series No. 131, American Chemical Society, Washington, D.C., 1974, pp 108-125.

TABLE 1. TEST CONDITIONS FOR TYPICAL TESTS

Test Number	Total Coal, lbm	Duration, seconds	Flowrates, lbm/sec			Average Temperatures, F			Injector
			Coal	H_2	O_2	Wall	Reactor	Calculated Reactor	
23	19.7	234	0.084	0.0383	0.0226	1780	1780	1830	4-on-1
24	15.6	210	0.074	0.0380	0.0230	1820	1700	1920	
25	17.0	155	0.110	0.0372	0.0149	1430	1400	1590	
26	19.2	240	0.080	0.0386	0.0196	1550	1500	1770	

NOTES: (1) Tests 23, 24, and 26 were made with oxygen injection in the reactor.
(2) Test 25 was made with oxygen injection in the preburner.
(3) Calculated reactor temperatures correspond to mixing with no heat of reaction.

TABLE 2. COMPOSITION OF COAL, CHAR AND LIQUID PRODUCT FROM TYPICAL TESTS

Constituent	Composition, percentage by weight					
	Coal	Raw Char				Benzene Extractable Material
		Test 23	Test 24	Test 25	Test 26	
Moisture	2.05	2.83	5.96	7.49	5.17	
Ash	10.56	18.54	18.95	14.71	15.89	
Carbon	69.25	69.97	67.15	67.94	71.01	85.70
Hydrogen	4.87	2.82	2.64	2.78	2.66	5.67
Nitrogen	1.46	0.58	0.71	1.38	0.95	1.08
Chlorine	0.01	0.01	0.01	0.02	0.01	
Sulfur	4.26	3.28	3.11	3.16	2.65	
Oxygen (Diff.)	7.54	1.97	1.47	2.52	1.66	
Benzene Extractable Fraction	0.5	15.5	9.9	18.3	23.2	

TABLE 3. COMPOSITION OF PRODUCT GAS FROM TYPICAL TESTS

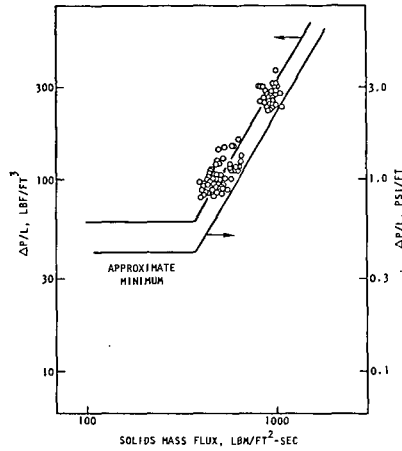| Component	Mole Fraction, percent			
	Test 23	Test 24	Test 25	Test 26
N_2	2.6	0.9	1.3	2.5
H_2	89.4	91	93	89
CO	4.7	3.4	0.3	1.8
CO_2	0.2	0.2	0.1	0.1
CH_4	2.2	4.0	1.6	1.1
C_2H_4	-	<0.1	<0.1	<0.1
C_2H_6	0.2	0.1	0.4	0.2
C_3H_8	-	-	<0.1	-
C_4H_{10}	-	-	-	-
Benzene	$7.7(10^{-4})$	$7.3(10^{-4})$	$2.5(10^{-4})$	$5.1(10^{-4})$
Toluene	$3.8(10^{-5})$	$1.3(10^{-5})$	$1.3(10^{-4})$	$4.8(10^{-5})$
Xylene			$2.8(10^{-5})$	$1.2(10^{-6})$

Figure 1.   Measured Transport Line Pressure Gradient
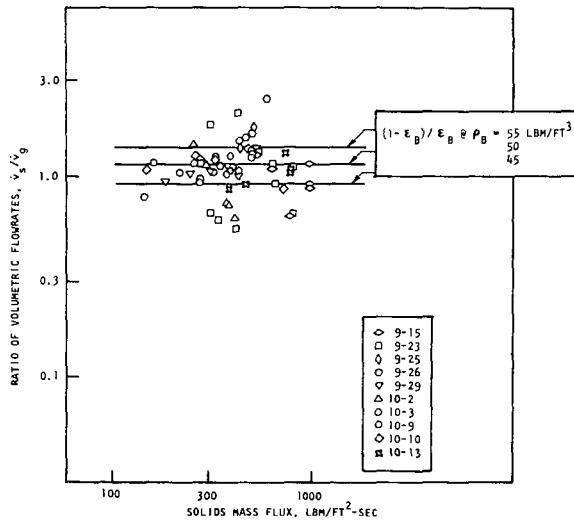Obtained From Mixing Test Facility

Figure 2.   Ratio of Solid-to-Gas Volumetric Flowrates
Obtained From Transparent Feeder Data

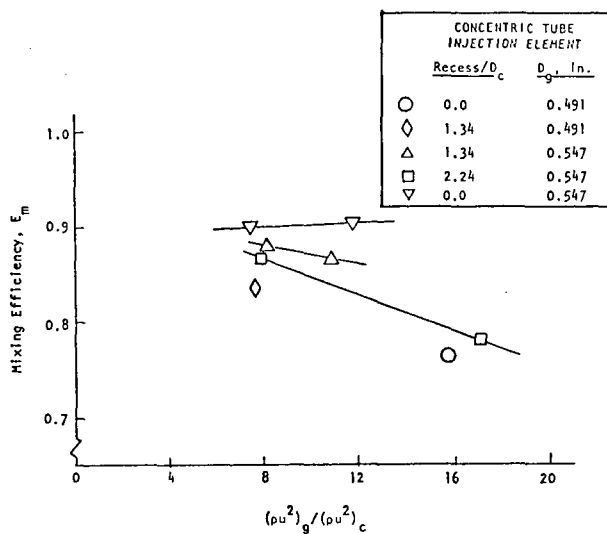Figure 3.   Cold-Flow Mixing Results From Concentric Tube
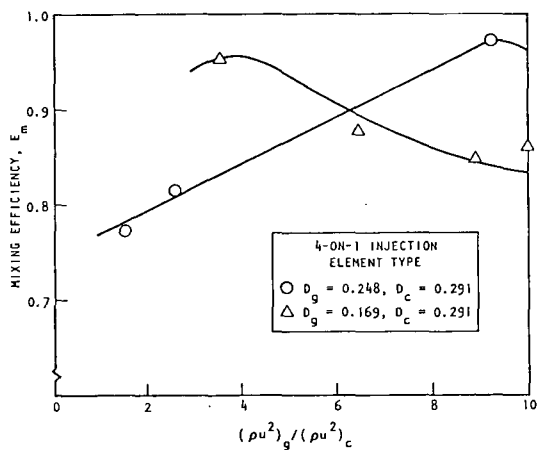   Injection Elements

Figure 4.   Cold-Flow Mixing Results From 4-on-1
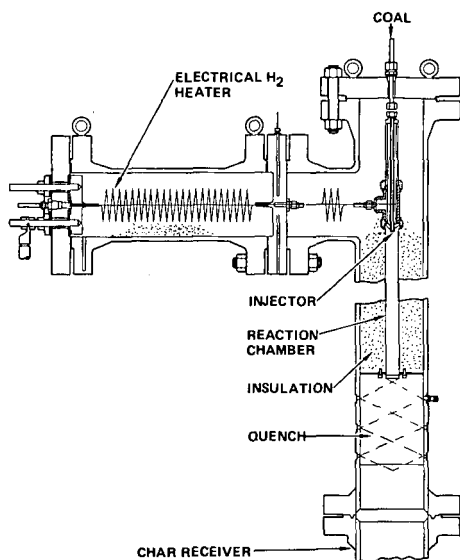   Injection Elements

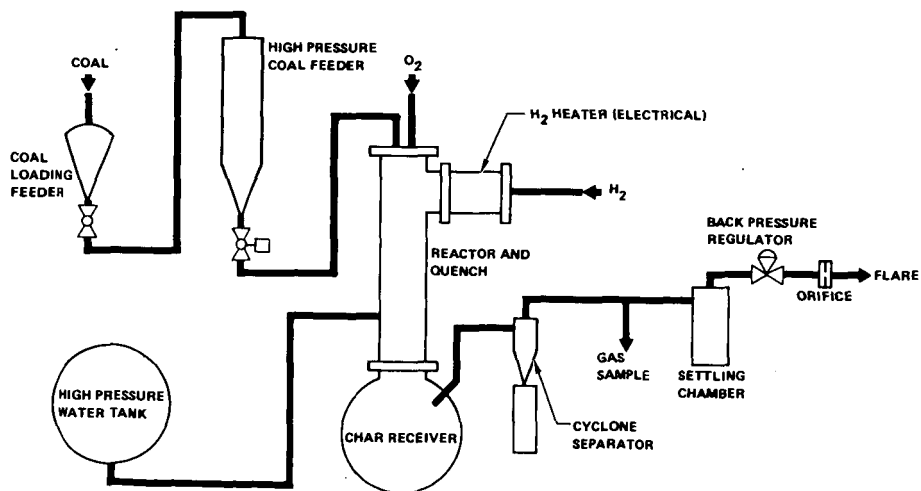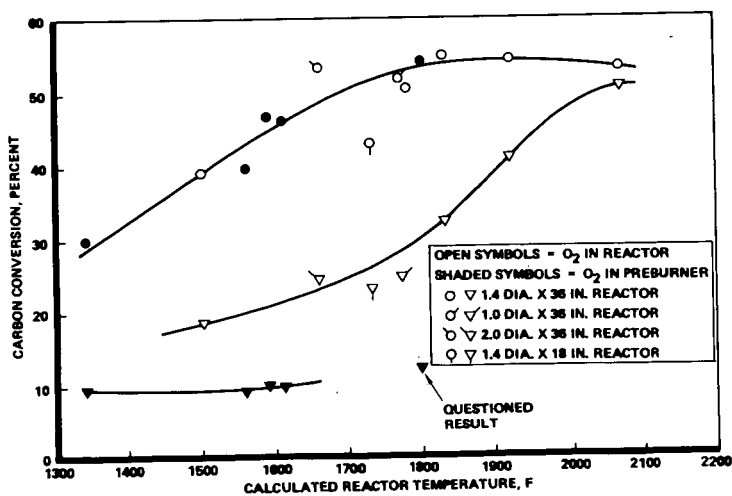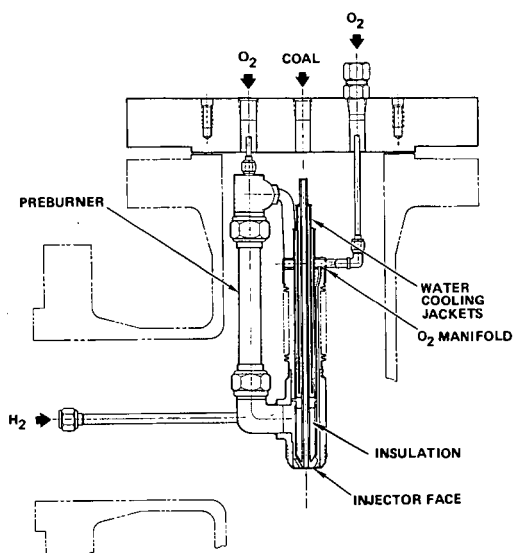Figure 5.   Schematic Diagram of 0.2-tph Reactor Assembly

Figure 6.   Flow Diagram of 0.2-tph Reactor Test System

194

Figure 7.   0.2-tph 4-on-1 Injector and Preburner With
            Oxygen Injection Capability

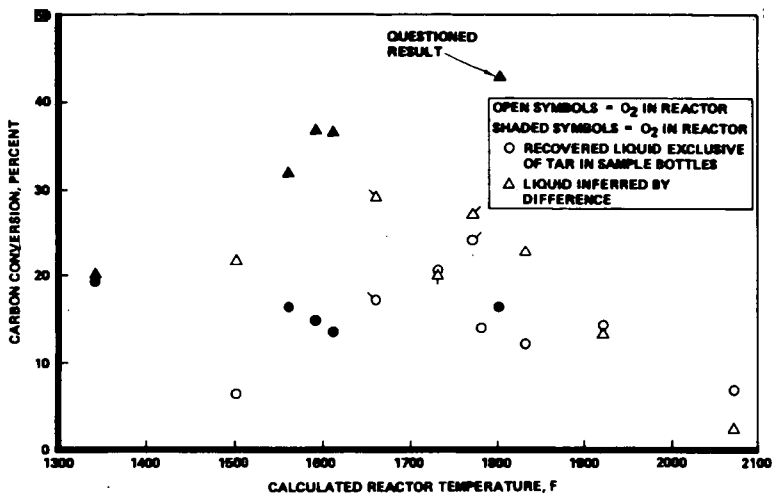Figure 8.   Carbon Conversion Results From 0.2-tph Reactor Testing

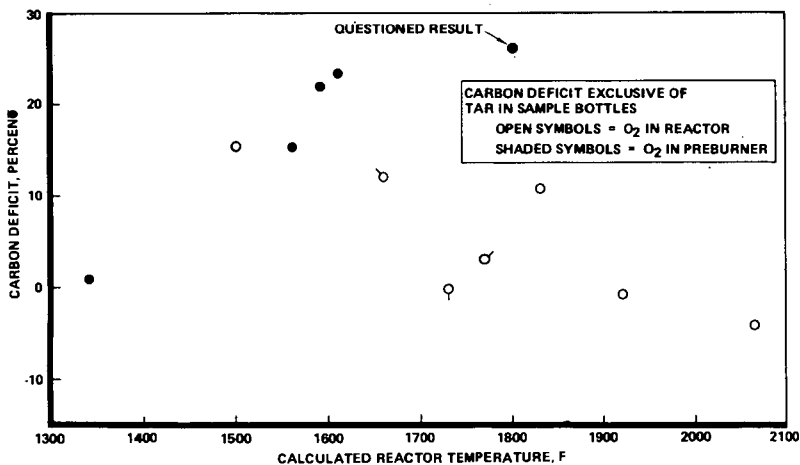Figure 9. Carbon Conversion to Liquids From 0.2-tph Testing

Figure 10. Carbon Deficit in Products From 0.2-tph Testing